Rheology and Interparticle Interaction Studies in Complex Media

Prasad S. Bhosale

A dissertation

submitted in partial fulfillment of the

requirements for the degree of

Doctor of Philosophy

University of Washington

2012

Reading Committee:

John C. Berg, Chair

Rene Overney

Brain Hayes

Program Authorized to Offer Degree:

Chemical Engineering

University of Washington

Abstract

Rheology and Interparticle Interaction Studies in Complex Media

Prasad S. Bhosale

Chair of the Supervisory Committee:
Professor John C. Berg
Department of Chemical Engineering

Dense colloidal dispersions are rheologically complex and exhibit properties like yield stress, creep, and elasticity due to aggregation and other interparticle interactions. The overall rheological performance of the system is due to the multiscale properties and mechanics: the nanoscale interactions between particles determine the microscopic texture, i.e. aggregate compactness, structure and strength. At microscale the micromechanics and microstructure evolution in aggregates under stress define the macroscale rheological performance. The interparticle forces and microstructure also evolve over time (aging interparticle bonds and aggregate structures), leading to time/frequency dependent rheological behavior.

The systems of specific interest here are dense nuclear waste slurries stored at the US Department of Energy sites at Hanford, WA and Savannah, GA since 1943. Rheological modifiers are currently being investigated for effective transport of these dense waste slurries in the vitrification process developed for more permanent radioactive waste disposal. The overall objective of the study is to fundamentally

understand the performance of rheology modifiers in environments similar to those of nuclear waste slurries. We are particularly focused on the effect of rheology modifiers on interparticle interactions and its implication towards bulk rheological performance. These interactions were investigated through various macroscale (rheology and electroacoustics) and microscale (atomic force microscope) colloidal interaction measurement techniques. The implications of these interactions towards rheological performance are studied using the simple yield stress model defined by Russel et al. Here the model has been extended to steric, and bridging forces between particles.

It was identified that polyelectrolytes, specifically poly (acrylic acid), is an effective rheology modifier for high pH and high salt content environments of nuclear waste slurries. The correct choice of molecular weight of the PAA was especially important to its effectiveness: too low a value provides insufficient steric stabilization, while too high a value induces bridging. The effect of poly (acrylic acid) adsorption on the electrokinetic behavior of alumina dispersions under high pH conditions was also investigated as a function of polymer concentration and molecular weight as well as the presence, concentration and ion type of background electrolyte. The interparticle interaction forces were directly measured in nuclear waste simulant using atomic force microscopy. A link between the dynamics of polymer bridging and disruption and bulk rheology was established for a model dense colloidal suspension of silica particles flocculated by polyethylene oxide (PEO). In the finial study, as a side project, we have expanded acoustic spectroscopy and electroacoustic techniques to characterize particles dispersed in viscoelastic polymer gel media (another complex system of interest).

TABLE OF CONTENTS

LIST OF FIGURES

LIST OF TABLES

ACKNOWLEDEMENTS

Many thanks to Professor John C. Berg for all of his help. I especially thank him for freely sharing his knowledge, and wisdom, and for patiently teaching me to effectively write about scientific research. All of the members of Professor Berg's research group contributed in some way to this work. I would like to thank my family and friends who have been a great support. Finally, I acknowledge the financial support of the Department of Energy (EM-30 project) and our collaborators at Pacific Northwest National Lab.

INTRODUCTION

Dense colloidal dispersions are encountered in a wide verity of industrial applications; for example: waste treatment,[1,2] ceramic processing,[3] mining,[4] food processing, pharmaceuticals[1] etc. Often these suspensions are rheologically complex. They exhibit viscoelastic properties including yield stresses, creep, due to particle aggregation and other interparticle interactions.[5,6] The overall rheological performance of the colloidal suspensions is due to the multiscale properties and mechanics: Nanoscale interactions between particles determine the microscopic texture, i.e. aggregate compactness, structure and strength.[7] At the microscale, the micromechanics of aggregates and microstructure evolution under stress define the macroscale rheological performance. The interparticle interactions and microstructure also evolve over time (aging interparticle bonds and aggregate structures) leading to time/frequency dependent rheological behavior.[8,9] A clear understanding of rheological performance is crucial while carrying out the transport and handling of these fluids.

The systems of specific interest here are dense nuclear waste slurries, stored at the US Department of Energy sites at Hanford, WA and Savannah, GA since 1943. As the storage tanks for these slurries are beginning to fail, vitrification facilities are being developed for more permanent disposal. The slurries are multi-component, dense (25 to 35 wt%) colloidal dispersions of particulates in the size range of 0.1 to 12

μm. The major solid components are aluminum hydroxides, zirconium hydroxides, ferrous hydroxides and silicon oxides residing in a strong basic environment (pH 12-13) with very high salt concentration (1.5-2M).[2] These dispersions show shear thinning behavior with a yield stress, τ_y. Rheology modifiers are being investigated to eliminate the yield stress and increase the allowable solid loading for effective transport in the vitrification processes. The dense suspensions may be envisioned as weakly aggregated or percolated particulate structures, as shown in Figure 1. As the yield stress is reached in the viscoelastic suspensions, inter-particle bonds in the aggregates are broken, and a sudden drop in viscosity is noted, followed by Newtonian or visco-plastic flow. If the suspension is subsequently unperturbed, aggregates can re-form, and the suspension can regain its yield stress and high apparent viscosity. In dense colloids, the yield stress is a direct manifestation of the inter-particle force F, and the number of particle–particle contacts per unit area perpendicular to the applied shear. Using the model suggested by Russel et al.[10] the latter should scale as ϕ^2/a^2, where ϕ is the volume fraction of the particles and a is the particle radius, i.e.:

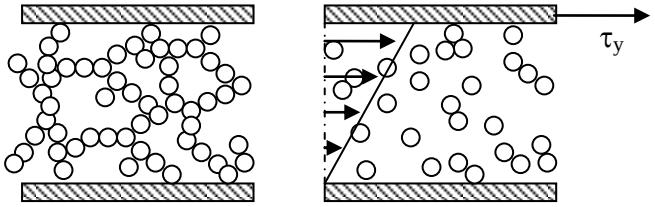

Figure 1: Cartoon representing breakdown of aggregates under shear.

$$\tau_y \propto \frac{\phi^2}{a^2} F \tag{1}$$

Russel et al.[10] defined the force F only in terms of repulsive electrostatic and attractive van der Waals forces:

$$F \approx \left(\frac{A_H}{12 D_o^2} - \frac{2\pi\varepsilon\varepsilon_o}{D_o} \zeta^2 \ln\left[\frac{1}{1-\exp(-\kappa D_o)} \right] \right) \tag{2}$$

where D_o is surface separation distance, A_H is the Hamaker constant, ε is the dielectric constant of the medium, ε_0 is the permittivity of free space, ζ is the particle zeta potential, and κ is the Debye parameter. Van der Waals forces are always present and strongly attractive at close enough proximity for the case of mineral oxide particles in water, while electrostatic forces in aqueous media are due to the counterion clouds surrounding the charged particle surfaces.

Most rheology modifiers are designed to alter interparticle forces to influence rheological performance. In many cases, the interactions between particles are not limited to electrostatic and van der Waals forces. Addition of polymeric modifiers can induce various types of interactions like steric (F_{steric}), bridging (F_{bridge}), depletion ($F_{\text{depletion}}$), and other forces (F_{other}), such as those of solvent structure or hydrophobic effects.[1] Thus:

$$F = F_{\text{vdW}} + F_{\text{elec}} + F_{\text{steric}} + F_{\text{bridge}} + F_{\text{depletion}} + F_{\text{other}} \tag{3}$$

Steric repulsion results when adsorbed polymer layers on approaching particles overlap producing osmotic pressure differences that seek to re-dilute the overlap

regions. Bridging occurs when dissolved polymers present in the system adsorb onto multiple particles. Attractive or repulsive depletion forces result when unadsorbed polymer molecules in the solution are excluded from space between particles due to large particle size. The resulting osmotic pressure difference forces the particle to flocculate or separate.

The overall interaction force *F* can be measured in various ways. At first, interparticle forces were measured indirectly through aggregation and sedimentation studies.[5, 11] For example, the Hamakar constant used for calculating van der Waals forces, was initially estimated by examining Brownian motion,[5] but the measurements were very crude. Suspension rheology was another indirect method employed to study interparticle forces. In these studies bulk rheological properties like viscosity, storage modulus, and yield stress of a simple and well characterized dispersion (low particle concentration, known particle size and shape, aggregate fractal number etc.) were correlated to interaction forces using mathematical models.[12-14] However, these correlations are often qualitative due to the large number of variables involved.[15] Later, advancement in electrokinetic techniques to measure electrophoretic mobility, zeta potential[5] and colloid vibration current (CVI) or electrosonic amplitude (ESA)[16] allowed one to accurately quantify electrostatic interactions. DLVO (Derjaguin and Landau, Verwey and Overbeek) theory combined the effects of the van der Waals and electrostatic interactions to describe forces between charged particles interacting through aqueous media.[5] In the last 25 years, development of the

surface force apparatus (SFA), and the atomic force microscope (AFM), have allowed direct measurements of surface/intermolecular forces and made tremendous impact in the field of colloidal science.[17-19] Not only electrostatic and van der Waals but various short and long range interactions (steric, briding, depletion, hydration etc.) have been investigated using these techniques. Recently, experiments using optical tweezers[9, 20-22] have elucidated micromechanics of aggregates and confocal microscopy experiments[23,24] with single particle tracking methods have shown microstructure evolution during flow. Experimental analysis at different length scales along with simulations[25] are now beginning lay down a complete picture for colloidal gel and suspension rheology.[4,25] Sophisticated analytical models have also been developed to accurately predict rheological properties like yield stress, viscosity etc. using nanoscale interparticle forces and microscale properties like fractal number and aggregate bending strength. However, these models are applicable only for well defined dispersions under rather moderate conditions (spherical monodispersed particles, low or moderate particle loading, Newtonian dispersing media, simple interparticle interactions etc.).[4, 21,26]

Industrially relevant suspensions are often not only dense, but involve complex environments like mixtures of different particles, strong acid/basic environments, high salt content, and the presence of polymers leading to viscoelastic suspending media. In such system interparticle interactions, microstructure and the effects of rheology modifiers on these properties are not well characterized. Therefore, the usual industrial

approach has been to select rheology modifier and "cook and look". A series of modifier types and dosages are tested to identify the most optimum rheological performance. Although such an approach can be an important first step, it requires rigorous and expensive experimentation, which is impractical in many situations. For example, in the case of nuclear waste slurries there is a danger of radioactive hazard, and experimentation is very tedious due to the different chemical compositions of each storage tank. There are 177 tanks in Hanford alone. Engineers at Pacific Northwest National laboratory have taken a somewhat more sophisticated approach. For each tank, a simulant representing the actual waste slurry was designed, and the rheology modifiers were tested with these simulants. The studies have identified poly(acrylic acid), and citric acid as effective modifiers.[2] However, there is lack of understanding regarding how and why these modifiers work in complex waste slurry environments.

The objective of this study is to fundamentally understand the performance of rheology modifiers in environments similar to those of nuclear waste slurries. A better understanding will help to improve modifier performance and ultimately allow us to design more effective modifier/modifier systems. We are particularly focused on the effect of rheology modifiers on interparticle interactions and its implication towards bulk rheological performance. These interactions were investigated through various macroscale (rheology and electroacoustics) and microscale (atomic force microscope) colloidal interaction measurement techniques. The implications of these interactions towards rheological performance are studied using the simple yield stress model

defined by Russel et al.[10] The model was initially designed for electrostatic and van der Waals forces only; however, its simplicity allows one to accommodate other types of interactions as mentioned above. Here the model has been extended to steric, and bridging forces between particles.

In our first study[1] (Chapter 1) we used bulk rheology measurement to investigate bridging and steric forces in dense alumina dispersions with poly(acrylic acid). Alumina is one of the major component in waste slurries, and recent studies[2] have identified poly (acrylic acid) (PAA) as a potential rheology modifier for such systems. These dispersions were studied in an environment similar to that of the nuclear waste slurries, viz., strong basic conditions (0.5N NaOH) with high salt concentrations (0.1–1M KNO_3). Electrostatic interactions can be neglected due to the high ionic strength. Polymer concentrations were very low, with a minimum of free polymer remaining in the solution, so that depletion effects could be neglected. Thus the overall interparticle force is composed of:

$$F = F_{vdW} + F_{steric} + F_{bridge} \quad (4)$$

It was found that the correct choice of molecular weight of the PAA was especially important to its effectiveness as a rheology modifier: too low a value provides insufficient steric stabilization, while too high a value induces bridging.

In the second study[27] (Chapter 2) we investigated electrokinetic properties of PAA coated alumina particles using electroacoustics. While electrostatic interactions between particles in such high ionic strength environments may be anticipated to be

negligible, a number of previous studies[17, 28] have shown them to be important even under such conditions. They become even more important as the nuclear waste slurry goes through dilution and concentration during processing cycles. The effect of poly (acrylic acid) adsorption on the electrokinetic behavior of alumina dispersions under high pH conditions was investigated as a function of polymer concentration and molecular weight as well as the presence, concentration and ion type of background electrolyte. The presence of all but the lowest molecular weight PAA studied (1800) led to decreases in dynamic electrophoretic mobility at low polymer and low salt concentrations, attributable to bridging flocculation. Bridging effects increased with polymer molecular weight, and decreased with polymer concentration. Increases in background electrolyte concentration enhanced dynamic electrophoretic mobility as the polymer layers were compressed and bridging was reduced. Such enhancements were reduced as the cation was changed from K^+ to Na^+ to Cs^+.

In the above two chapters, we studied modifier performance using indirect measurements like those of bulk rheology and electrokinetics. In the last 25 years, development of the surface force apparatus (SFA), and the atomic force microscope (AFM), have allowed direct measurements of surface/intermolecular forces and made tremendous impact in the field of colloidal science.[17-19] In the chapter 3, interparticle forces were directly measured using the atomic force microscope at conditions similar to those of nuclear waste slurries and we have sought to determine how a rheology modifiers will influence the interparticle interactions. We are especially interested in

AFM pull-off force measurements, which represent interparticle bond strength in an aggregate. The effects of salt concentration and the addition of PAA on adhesion forces were measured for alumina/sapphire and glass particle/SiO_2 systems. The adhesion forces between SiO_2 and alumina surfaces were also measured directly in the supernatant liquor from the nuclear waste simulant AZ101.

In chapter 4 we focus on the dynamics of particle contact. The dynamics of particle adhesion has practical implications for dense slurry transport. The particles can accumulate and aggregate in the dead zones (bends, elbows and pumps etc.) of the transport system, and if the particle contact sinter/age over time, then it is very difficult to remove these blockages. This is highly undesirable in nuclear waste slurry transport. The dynamics of polymer bridging and disruption and its effect on bulk rheology was studied for a model system of dense colloidal silica particle suspensions flocculated by polyethylene oxide (PEO). Microscale pull-off force measurements using atomic force microscope (AFM) show that upon repeated disruption and establishment of bridged contact, the adhesion between the surfaces is reduced. During contact disruption, the polymer chains bridging the two surfaces are stretched leading to chain scission. On the re-establishment of contact, these fragmented polymer chains are unable to fully re-establish the adhesion. Macroscale measurements using oscillatory rheology show that this reduced adhesion results in reduction of both the storage modulus and the yield stress. If the slurry is subjected to high shear for long

periods, polymer chain scission is amplified, and the fragmented polymer chains are unable to bridge the particles again, resulting in free flowing slurries.

Acoustic spectroscopy[16, 29] and electroacoustic[30] techniques are typically used to measure particle size distribution and electrokinetic properties in dense dispersions suspended in Newtonian media. In chapter 5, as a side project, we have expanded these techniques[1,31] to characterize particles dispersed in viscoelastic polymer gel media (another complex system of interest). The electroacoustics and acoustic attenuation of particles dispersed in polymer hydrogels was examined with the particle size either less than or greater than the gel mesh size. It was found that when the particles are smaller than the gel mesh size, their acoustic vibration is resisted by only the background water medium, and as the particle size is greater than the gel mesh size they experience frequency dependent viscoelastic response from the media.[1, 31] The degree of trapping, as varied by either decreasing mesh size at a constant particle size, or increasing particle size at a constant mesh size, did not alter the particle electrophoretic mobility below the critical storage modulus value *G'* (300 Pa). From a practical point of view these results show that electroacoustics and acoustic spectroscopy can be directly used to characterize un-trapped in viscoelastic gel media.

References

1. Bhosale, P. S.; Berg, J. C., Poly(acrylic acid) as a rheology modifier for dense alumina dispersions in high ionic strength environments. *Colloids Surf., A: Physicochem. Eng. Aspects* **2010,** 362, (1-3), 71-76.

2. Chun, J.; Poloski, A. P.; Hansen, E. K., Stabilization and control of rheological properties of $Fe_2O_3/Al(OH)_3$ -rich colloidal slurries under high ionic strength and pH. *Jr. Colloids & Int. Sci.* **2010,** 348, (1), 280-288.

3. Cesarano, J.; Aksay, I. A., Processing of highly concentrated aqueous α–alumina suspension stablized with polyelectrolytes. *J. Am. Ceram. Soc.* **1988,** 71, (12), 1062-1067.

4. Huynh, L.; Jenkins, P.; Ralston, J., Midifcation of the rheological properties of concentrated slurries by control of mineral-solution interfacial chemistry. *Int. J. Miner. Process.* **2000,** 59, 305-325.

5. Berg, J. C., *An Introduction to Interfaces and Colloids: The Bridge to Nanoscience*. World Scientific 2010; p p. 616.

6. Mewis, J.; Wagner, N. J., Current trends in suspension Rheology. *J. Non-Newtonian Fluid Mech.* **2009,** 157, 147-150.

7. Daintree, L.; Biggs, S., Particle-particle interactions: The link between aggergate properties and rheology. *Particulate Science and Technology* **2010,** 28, 404-425.

8. Manley, S.; Davidovich, B.; Davies, N. R.; Cipelletti, L.; Bailey, A. E.; Christianson, R. J.; Bowen, I. J.; Eggers, J.; Kurta, C.; Lorik, T.; Weitz, D. A., *Phys. Rev. Lett.* **2005,** 95, 048302.

9. Meng, B.; Wu, J.; Li, Y.; Lou, L., Aging process of the bond between colloidal particles. *Colloids Surf., A: Physicochem. Eng. Aspects* **2008,** 322, 253-255.

10. Russel, W. B.; Saville, D. A.; Schowalter, W. R., *Colloidal Dispersions*. Cambridge Press 1989.

11. Frens, G., Interacting Particles in Contact. *Faraday Discuss. Chem. Soc.* **1990,** 90, 143-151.

12. Johnson, S. B.; Franks, G. B.; Scales, P. J.; Healy, T. W., The binding of monovalent electrolyte ions on-Alumina II. The shear yield stress of concentrated suspensions. *Langmuir* **1999,** 15, 2844-2853.

13. Ducker, W. A.; Z. Xu; Clarke, D. R.; Israelachvili, J. N., Forces between alumina surfaces in salt solutions: Non-DLVO forces and implication for colloidal processing. *J. Am. Ceram. Soc.* **1994,** 77, 437-443.

14. Yilmaza, H.; Satoa, K.; Wataria, K., AFM interaction study of α-alumina particle and c-sapphire surfaces at high-ionic-strength electrolyte solutions. *Jr. Colloids & Int. Sci.* **2007,** 307, (1), 116-123.

15. Patina, J. P.; Furst, E. M., Micromechanics and contact forces of colloidal aggergates in the presence of surfactacts. *Langmuir* **2008,** 24, (4), 1141-1146.

16. Dukhin, A. S.; Goetz, P. J., *Ultrasound for characterizing colloids*. Elsevier: 2002; Vol. 15.

17. Fielden, M. L.; Hayes, R. A.; Ralston, J., Oscillatory and ion-correlation forces observed in direct force measurments between silica in concentrated $CaCl_2$ solutions. *Phys. Chem. Chem. Phys* **2000,** 2, 2623-2628.

18. Vakarelski, I. U.; Higashitani, K., Dynamic Features of Short-Range Interaction Force and Adhesion in Solution. *Jr. Colloids & Int. Sci.* **2001,** 242, 110-120.

19. Ralston, J.; Larson, I.; Rutland, M. W.; Feiler, A. A.; Kleijin, M., Atomic force miscroscope and direct surface force measurements. *Pure Appl. Chem.* **2005,** 77, (12), 2149-2170.

20. Pantina, J. P.; Furst, E. M., Colloidal aggergate micromechanics in the presence of divalent ions. *Langmuir* **2006,** 22, (12), 5282-5288.

21. Pantina, J. P.; Furst, E. M., Elasticity and critical bending moment of model colloidal aggergates. *Phys. Rev. Lett.* **2005,** 94, 138301.

22. Furst, E. M., Interactions, structure, and microscopic responce: Complex fluid rheology using laser tweezers. *Soft Materials* **2003,** 1, (3), 167-185.

23. Pickrahn, K.; Rajaram, B.; Mohraz, A., Relationship between microstructure, dynamics, and rheology in polymer-bridging colloidal gels. *Langmuir* **2009,** 26, (4), 2392–2400.

24. Mohraz, A.; Solomon, M. J., Direct visualization of colloidal rod assembly by confocal microscopy. *Langmuir* **2005,** 21, 5298-5306.

25. Lu, P. J.; Zaccarelli, E.; Ciulla, F.; Schofield, A. B.; Sciortino, F.; Weitz, D. A., Gelation of particles with short range attraction. *Nature* **2008,** 453, 499-503

26. Franks, G. V.; Zhou, Y.; Yan, Y.-d.; Jameson, G. J.; Biggs, S., Effect of aggergate size on sediment bed rheological properties. *Phys. Chem. Chem. Phys* **2004,** 6, 4490-4498.

27. Bhosale, P. S.; Chun, J.; Berg, J. C., Electrophoretic mobility of poly(acrylic acid)-coated alumina particles. *Jr. Colloids & Int. Sci.* **2011,** 258, 123-128.

28. Stenkamp, V. S.; McGuiggan, P.; Berg, J. C., Restabilization of Electrosterically Stabilized Colloids in High Salt Media. *Langmuir* **2001,** 17, (3), 637-651.

29. Dukhin, A. S.; Goetz, P. J., Acoustic Spectroscopy for Concentrated Polydisperse Colloids with Density Contrast. *Langmuir* **1996,** 12, (21), 4987-4997.

30. O'Brien, R. W., Electro-acoustic effects in a dilute suspension of spherical particles. *J. Fluid Mech.* **1988,** 190, 71-86.

31. Bhosale, P. S.; Chun, J.; Berg, J. C., Electroacoustics of particles dispersed in polymer gel. *Langmuir* **2011,** 27, (12), 7376-7379.

CHAPTER 1

Poly (acrylic acid) as a Rheology Modifier for Dense Alumina Dispersions

1.1 Introduction

Radioactive nuclear waste slurries are rheologically complex since the particulates that compose them can aggregate, forming microstructures of various types that can induce solid-like behavior.[1-3] Recently, poly(acrylic acid) (PAA) was found to be a promising candidate for reducing the yield stress and viscosity of these waste slurries, of which aluminum hydroxides are a major component.[2] This chapter is focuses on PAA addition to dense alumina dispersions stored in an environment similar to that of the nuclear waste slurries, viz., strong basic conditions (0.5M NaOH) with high salt concentrations (0.1-1M KNO_3) for purposes of rheology modification. To the best of our knowledge, poly (acrylic acid) has not been studied as a dispersant in media beyond 0.1M in ionic strength, and in particular, the important variable of molecular weight has not been investigated under these conditions. Increasing the ionic strength screens the electrostatic forces between COO^- groups, allowing PAA chain collapse,[4] and it is likely that this collapse is not complete even at 0.1M ionic

strength. Furthermore, studies involving other colloids in high salt media have revealed a number of unusual effects.[5]

Dense alumina suspensions show shear thinning behavior with a yield stress, τ_y. The yield stress is a direct manifestation of the inter-particle force F, and the number of particle-particle contacts per unit area.[1, 6] Most rheological modifiers are designed to alter the inter-particle interaction force, which is in general composed of van der Waals (F_{vdW}),[7] electrostatic (F_{elec}),[1] steric (F_{steric}),[8] bridging (F_{bridge}),[9] depletion ($F_{depletion}$)[8] and other components (F_{other}), for example those of solvent structure or hydrophobic effects.[1] Electrostatic forces are effectively screened out and negligible in high enough ionic strength environments.[1] Attractive depletion forces result from the presence of unadsorbed polymer.[8] In the systems under study, depletion effects may be neglected due to low free polymer concentration. Finally, neither solvent structuring nor hydrophobic effects are expected to play a significant role, so that to good approximation for the systems under study,

$$F = F_{vdW} + F_{steric} + F_{bridge}. \qquad 1.1$$

van der Waals forces are always present and strongly attractive at close enough proximity for the case of mineral oxide particle in water. Steric repulsion results when adsorbed polymer layers on approaching particles overlap producing osmotic pressure differences that seek to re-dilute the overlap regions. Bridging occurs when dissolved polymers present in the system adsorb onto multiple particles. The decisive factor in determining the net inter-particle attraction is usually just the relative magnitude van

der Waals attraction and steric repulsion, which depends on the inter-particle spacing, S_0, which corresponds roughly to twice the polymer adlayer thickness, i.e. 2δ. When this is large enough, the net attractive forces are zero, and the colloid is stable against aggregation.

The adlayer thickness depends on the extension of the adsorbed polymer molecules from the particle surface, which in turn depends on the polymer molecular weight and its degree of solvency in the medium. For purposes of yield stress reduction it would thus appear that the higher MW polymer the better, but when the chain extension becomes too great, polymer bridging can induce aggregation and thus increase the yield stress.[4-5, 10-11] Figure 1.1 represents the effect of changing the polymer molecular weight. While the degree of polymer chain extension depends primarily on its molecular weight, it is also influenced by its solvency, which depends on the salt concentration. PAA molecules are known to undergo significant conformation changes over the range of monovalent salt concentrations of 0.01 to 2 M, and the adsorption of PAA onto metal oxide surfaces is also increased at high ionic strengths due to the decrease in solvency.[12-13] In the vitrification process, nuclear waste slurries go through dilution and concentration cycles. Thus in order to evaluate PAA as a dispersant in slurries relevant to the radioactive tank wastes, here we examined the stability and rheological behavior of dense alumina slurries over a wide PAA molecular weight range (1800 to 4 x 10^6 g/mol) at a concentration of 0.717 mg/m^2 (0.3 wt% of alumina) in media of high salt concentration (0.1-1M KNO_3) and pH corresponding to the presence of 0.5M NaOH.

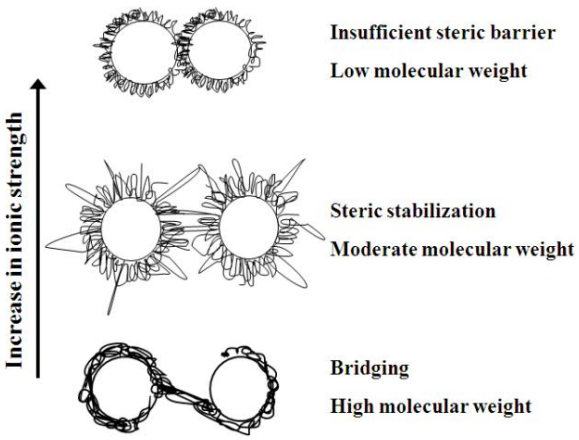

Figure 1.1: Schematic of the different interaction mechanisms observed with change in the PAA molecular weight and ionic strength.

1.2 Poly (acrylic acid) Adsorption Isotherms

Figure 1.5 shows the PAA 90 kg/mol-alumina adsorption isotherms measured at different KNO_3 concentrations (0.1M, 0.5M and 1M) in 0.5M NaOH solution. An increase in adsorption with an increase in the ionic strength was observed. The reduced solubility of polymer at high ionic strengths leads to higher adsorption. The optimum PAA concentrations for dispersing alumina corresponded to the inception of the knee in the adsorption isotherm.[14-15] In the systems under study, this occurred approximately at a value of 0.5 mg/m^2. The poly (acrylic acid) dosage selected was 0.717 mg/m^2 which insured full coverage of alumina particles surfaces,[10, 12] but with a minimum of free polymer remaining in the solution, so that depletion effects[16] could avoided.

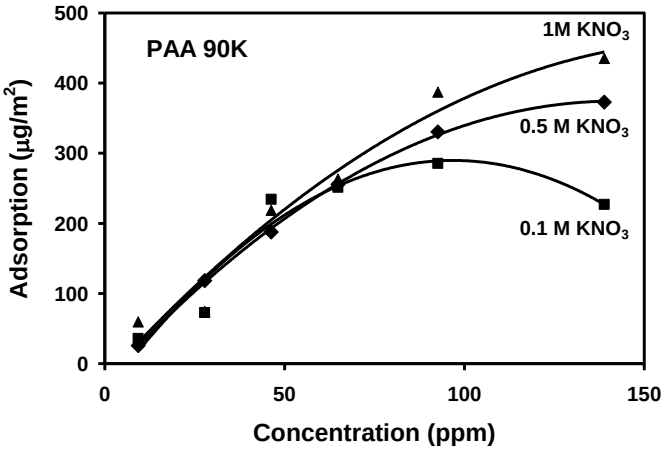

Figure 1.2: Adsorption isotherms for PAA 90 kg/mol on alumina at 0.1M, 0.5M, and 1M KNO_3 concentration in 0.5M NaOH solution.

1.2 Optimum Molecular Weight

It was found that the correct choice of molecular weight of the PAA was especially important to its effectiveness as a rheology modifier: too low a value provides insufficient steric stabilization, while too high a value induces bridging. Figure 1.2 shows viscosity vs. shear stress plots obtained for different PAA molecular weights, with the KNO_3 concentration maintained at 0.5M (1M total ionic strength, 0.5M K^+ ions and 0.5M Na^+ ions). The addition of 1.8, 5, 50 and 90 kg/mol MW PAA all produced yield stress (τ_y) values roughly comparable to those of the pure alumina dispersion, while a molecular weight of 200 kg/mol produced a significant decrease in the yield stress. In contrast, a PAA molecular weight of 450 kg/mol more than doubled the yield stress, due to bridging.

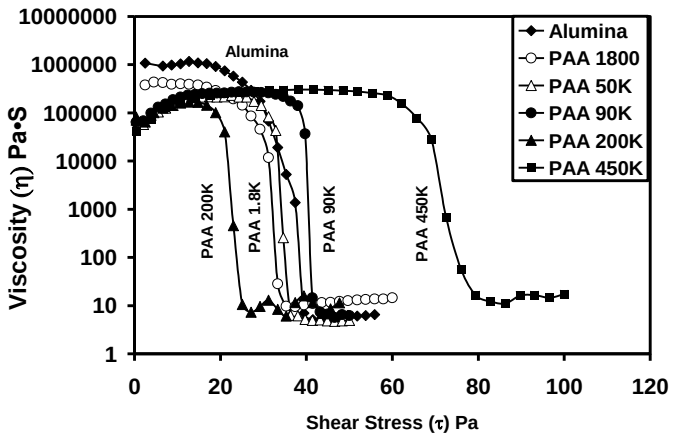

Figure 1.3: Viscosity (η) vs. shear stress (τ) for 34.65 vol% alumina slurries in a 0.5M NaOH, 0.5M KNO_3 solution with PAA molecular weights of 50, 90, 200 and 450 kg/mol (50K, 90K, 200K and 450K respectively). PAA concentration was maintained at 3 mg/g of alumina for all PAA molecular weights.

1.3 Effect of Ionic Strength

PAA adsorption on metal oxide surfaces is known to be significantly influenced by the ionic strength of the solution.[14-15,20] The molecular weight that produced the greatest reductions in slurry yield stress depended on the ionic strength of the medium. Figure 1.3 shows the effect of PAA conformational changes on the rheology of the alumina slurries in terms of relative yield stress vs. ionic strength for PAA molecular weights of 90 and 200 kg/mol. The relative yield stress is the ratio of the yield stress in the presence of polymer (τ_{yPAA}) to the yield stress observed in its absence (τ_y) at the same KNO_3 concentration level. Among the systems and conditions investigated, optimum yield strength reductions of approximately 40% (compared with comparable slurries in the absence of polymer) were achieved with a PAA

molecular weight of 90 kg/mol in 0.1M KNO_3 media, but 200 kg/mol in 0.5M KNO_3. For 1M KNO3, the apparent optimum would be between 200 and 450 kg/mol.

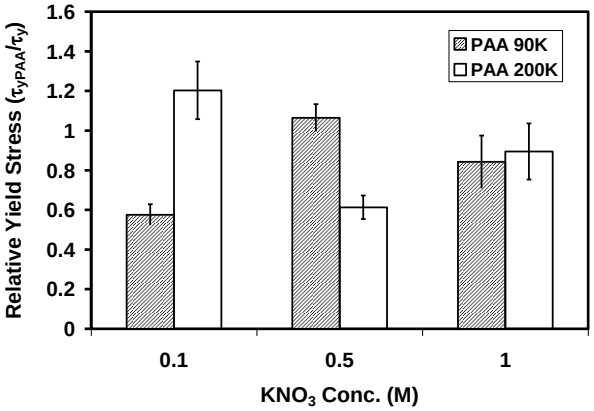

Figure 1.4: Change in relative yield stress for alumina-PAA system (90 and 200 kg/mol) at different KNO_3 concentrations.

The change in optimum molecular weight with salt concentration was due to conformational changes in the PAA molecules. PAA in basic environments with moderate ionic strength (0.1M) is in a partially stretched conformation due to intra-molecular electrostatic repulsive forces between carboxylate ($–COO^-$) groups.[4] Increases in ionic strength screen these forces[4] and decrease the PAA solubility,[12] both of which allow the PAA chains to fold upon themselves and collapse, decreasing adlayer thickness. To corroborate the expected changes in PAA conformation with ionic strength, the hydrodynamic radii of the PAA molecules in 0.5N NaOH, KNO_3 solutions of varying KNO_3 concentration were studied using dynamic light scattering (DLS). Figure 1.4 shows the expected sharp decreases in the hydrodynamic radius of PAA 1×10^3 and 450 kg/mol with ionic strength.

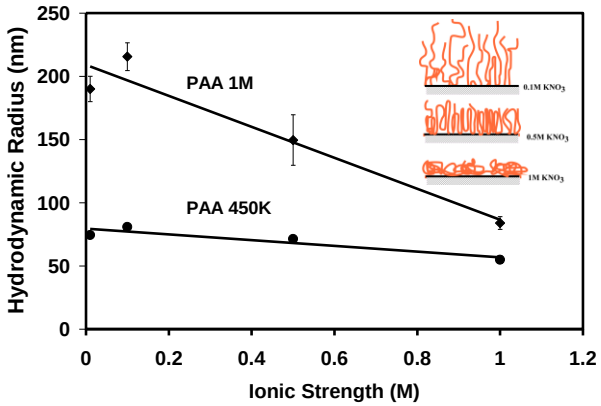

Figure 1.5: Change in hydrodynamic radius of free PAA MW 1×10^3 and 450 kg/mol molecules vs. KNO_3 concentration in 0.5N NaOH, as measured by dynamic light scattering. Inset: schematic of adlayer change with increasing ionic strength.

1.4 Summary

Rheology modification of dense alumina dispersions in highly basic media (0.5M NaOH) using poly (acrylic acid) (PAA) was investigated as a function of polymer molecular weight and solution ionic strength (0.1-1M KNO_3). Significant reductions in yield stress and viscosity could be achieved if the PAA molecular weight was high enough to produce robust steric repulsion, but not so high that bridging flocculation resulted. The particular molecular weight that produced the greatest reductions in slurry yield stress depended on the ionic strength of the medium. Among the systems and conditions investigated, optimum yield strength reductions of approximately 40% (compared with comparable slurries in the absence of polymer) were achieved with a PAA molecular weight of 90 g/mol in 0.1M KNO_3 media, but 200 kg/mol in 0.5M KNO_3. For 1M KNO3, the apparent optimum would be between 200 and 450 kg/mol.

References

1. Berg, J. C., *An Introduction to Interfaces and Colloids: The Bridge to Nanoscience*. World Scientific 2010; p p. 616.

2. Chun, J.; Poloski, A. P.; Hansen, E. K., Stabilization and Control of Rheological Properties of Fe2O3-rich Colloidal Slurries under High Ionic Strength and pH. *Jr. Colloids & Int. Sci.* **2010,** 348, (1), 280-288.

3. Chang, H. O., *Hazardous and radioactive waste treatment technologies handbook*. CRC Press LLC: Florida, 2001.

4. Sarkar, D.; Somasundaran, P., Conformational dynamics of poly(acrylic acid). A study using surface plasmon resonance spectroscopy. *Langmuir* **2004,** 20, (11), 4657-4664.

5. Stenkamp, V. S.; McGuiggan, P.; Berg, J. C., Restabilization of Electrosterically Stabilized Colloids in High Salt Media. *Langmuir* **2001,** 17, (3), 637-651.

6. Russel, W. B.; Saville, D. A.; Schowalter, W. R., *Colloidal Dispersions*. Cambridge Press 1989.

7. Israelachvili, J. N., *Intermolecular and Surface Forces*. Third ed.; Academic Press: 2011.

8. Napper, D. H., *Polymeric stabilization of colloidal dispersions*. Academic Press Inc.: New York, 1983.

9. Fleer, G. J.; Cohen Stuart, M. A.; Scheutjens, J. M. H. M.; Cosgrove, T.; Vincent, B., *Polymers at interfaces*. Chapman & Hall Inc.: New York, 1993.

10. Das, K. K.; Somasundaran, P., Ultra-low dosage flocculation of alumina using polyacrylic acid *Colloids Surf., A* **2001,** 182, 25-33.

11. Das, K. K.; Somasundaran, P., Flocculation-dispersion characteristics of alumina using a wide molecular weight range of polyacrylic acids. *Colloids Surf., A* **2003,** 223, 17-25.

12. Chibowski, S.; Mazur, E. O.; Patkowski, J., Influence of ionic strength on the adsorption properties of the system dispersed aluminium oxide-polyacrylic acid. *Mater. Chem. Phys.* **2005,** 93, 262-271.

13. Chibowski, S.; Wiśniewska, M., Study of the adsorption mechanism and structure of adsorbed layers of polyelectrolytes at metal oxide/solution interface. *Adsorpt. Sci. Tech.* **2001,** 19, (5), 409-421.

14. Cesarano, J.; Aksay, I. A., Processing of highly concentrated aqueous α–alumina suspension stablized with polyelectrolytes. *J. Am. Ceram. Soc.* **1988,** 71, (12), 1062-1067.

15. Palmqvista, L.; Lyckfeldta, O.; Carlströma, E.; Davoustb, P.; Kauppic, A.; Holmbergd, K., Dispersion mechanisms in aqueous alumina suspensions at high solids loadings. *Colloids Surf., A* **2006,** 274, 100-109

16. Miling, A. J.; Vincent, B., Depletion forces between silica surfaces in solution of poly(acryic acid) *J. Chem. Soc., Faraday T rans.* **1997,** 93, (17), 3179-3183.

CHAPTER 2

Electrophoretic Mobility of Poly (acrylic acid)-Coated Alumina Particles

2.1 Introduction

Polyelectrolytes are commonly used to flocculate, stabilize, or lubricate dispersed particles in industrial processes such as filtration, dip coating, waste water treatment, ceramic casting, etc.[1-5] The electrical properties of polymer-coated particles are critical to such processes,[6] and their electrokinetic behavior has been studied extensively.[7-14] While non-ionic polymers adsorbed on charged particle surfaces simply shift the hydrodynamic slip plane outward, reducing the surface charge at the slip plane and correspondingly the electrophoretic mobility,[8, 11, 13] the case of particles coated with polyelectrolytes is more complicated, as both the particle surfaces and the polyelectrolyte carry charge.[14-16]

Rheological[17-18] studies have identified a polyelectrolyte, poly (acrylic acid) (PAA), as a potential rheology modifier for nuclear waste slurries which are stored in strong basic environments (pH 12-12.5), and high ionic strength (0.5-1.5M) arising from the presence of various types of electrolytes. In chapter 1 we have shown that the correct choice of molecular weight (MW) of the PAA is critical to its effectiveness as a rheology modifier, with an optimum MW minimizing yield stress and viscosity. While electrostatic interactions between particles in such high ionic strength environments may be

anticipated to be negligible, a number of previous studies have shown them to be important even under such conditions.[13-14] They become even more important as the nuclear waste slurry goes through dilution and concentration during processing cycles.

Therefore, understanding the effects of poly (acrylic acid) adsorption on the electrical properties of particles under given conditions is important. Electrophoretic mobility measurements, both dc and acoustic, provide convenient means of estimating the electrical properties of colloidal particles. In the case of polymer-coated particles, such measurements can provide insights into many important colloidal properties, such as polymer adlayer thickness, the change in net surface charge by[8] polyelectrolyte adsorption and the apparent shift in the slip plane by the polymer adlayer.[7,9-10,12] Dynamic (acoustic) electrophoretic mobility measurements are also sensitive to change in particle size distribution (PSD) due to aggregation or bridge flocculation. However, the conventional electrophoresis in relatively high salt concentrations conditions and for large primary particles, i.e. in the Helmholtz-Smoluchowski conditions (κa>100), will lead to mobility's that are independent of particle size and thus reflect only the surface electrical properties. The objective of this study was to use both steady static (dc) and dynamic (acoustic) electrophoretic mobility measurements to probe the effects of poly (acrylic acid) adsorption on the electrical properties of colloidal alumina particles under a variety of conditions relevant to nuclear waste processing. Specifically, the effects of poly (acrylic acid) PAA, in high salt, high pH, dense alumina dispersions were examined as a function of polymer molecular weight and concentration, background electrolyte concentration (0 to 0.5M) and salt type ($LiNO_3$, $NaNO_3$, KNO_3 and $CsNO_3$).

2.2 Poly (acrylic acid) Dosage and Molecular Weight

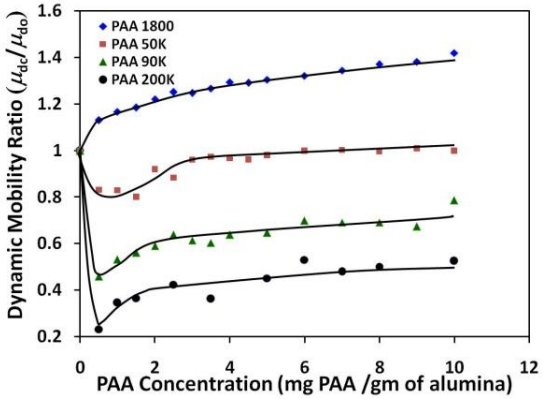

Figure 2.1: Change in dynamic electrophoretic mobility ratio (μ_{dc}/μ_{do}) of alumina particles measured by acoustic electrophoresis with addition of poly (acrylic acid) different molecular weight (1800, 50K, 90K and 200K) at pH 12 (20 mM NaOH). The lines drawn are to guide the eye.

Figure 2.1 shows the change in mobility ratio (μ_{dc}/μ_{do}), the ratio of the dynamic mobility of the PAA-coated particles (μ_{dc}) to the dynamic mobility of the bare particles (μ_{do}), with PAA concentration and MW from 1800 to 200K. Adsorption of the lowest MW PAA studied, 1800, increased the μ_{dc} of the particles in dense dispersions, in proportion to the polymer concentration, gradually reaching an increase of 40% over that of the bare particles as adsorption saturation was approached. The effect of the PAA 1800 adsorption was thus to increase the particle surface charge density. Adsorption of PAA of higher MW (from 50K to 200K) produced decreases in the dynamic electrophoretic mobility that were greatest at the lowest polymer concentrations, and became smaller as concentration increased and plateau adsorption was approached. The extent of the decreases in dynamic electrophoretic mobility occurred in direct proportion to the polymer MW at all concentrations. These results are consistent with the occurrence of bridging flocculation. In contrast, the measured conventional dc electrophoretic mobility in dilute dispersions, which was not influenced by any possible bridging, was the same

for all polymer molecular weights up to 1M at adsorption saturation, as shown in Figure 2.2.

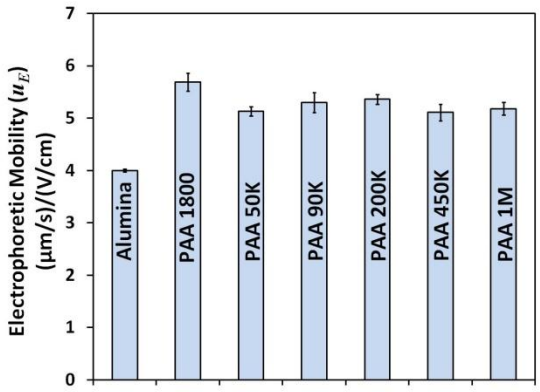

Figure 2.2: Electrophoretic mobility (u_E) of alumina particles measured by laser Doppler electrophoresis with different poly (acrylic acid) molecular weight (1800, to 1M) at pH 12 (20 mMNaOH) and 10 mg PAA/gm alumina.

2.3 Ionic Strength and Ion Type

Increasing concentration of background electrolyte (from 0 to 0.5M KNO_3) produced increases in apparent dynamic electrophoretic mobility at all polymer concentrations as the increased electrostatic screening lead to a more compressed polymer and reduced bridging. At the highest electrolyte concentration (0.5M KNO_3), the dynamic electrophoretic mobility *vs.* polymer concentration collapsed into a single curve for all polymer molecular weights, including 1800, as shown in Figure 2.3, for which no bridging occurred at any electrolyte concentration.

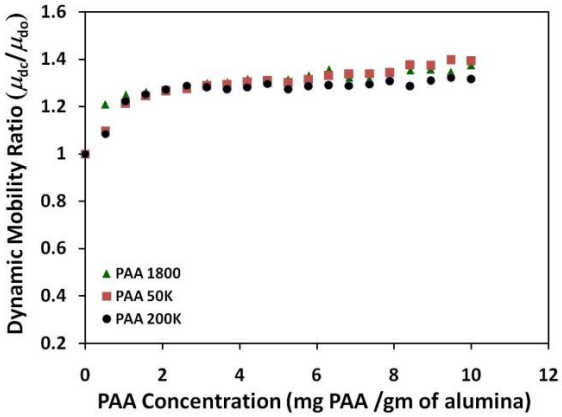

Figure 2.3 Change in dynamic electrophoretic mobility ratio (μ_{dc}/μ_{do}) of alumina particles measured by acoustic electrophoresis with addition of different poly(acrylic acid) molecular weight (1800, 50K and 200K) at 0.5M KNO_3 and pH 12 (20 mM NaOH).

The influence of background electrolyte on dynamic electrophoretic mobility, and by inference on polymer bridging, was found to depend on cation type. Nuclear waste slurry contains different types of electrolytes with cations such as K^+, Na^+, and Cs^+. PAA adsorption increases with increasing salt concentration even at high salt concentrations due to solubility (salting out) effects,[15-16] so one might expect such effects to be salt specific (Hofmeister series). The hydrated cations have different sizes ($Li^+ > Na^+ > K^+ > Cs^+$). Figure 2.4 shows the dynamic electrophoretic mobility ratio at 0.5M salt concentration for PAA-coated alumina particles with different cation types. The relative enhancement of mobility caused by polymer adsorption decreased from Na^+ to K^+ to Cs^+. In fact, for PAA MW 200K, there was a *decrease* in relative mobility, evidently attributable to bridging. The PAA chains and were not completely collapsed even at 0.5 M Cs^+ concentration, i.e., salting-out effects are weaker than in the cases of Na^+ or K^+.

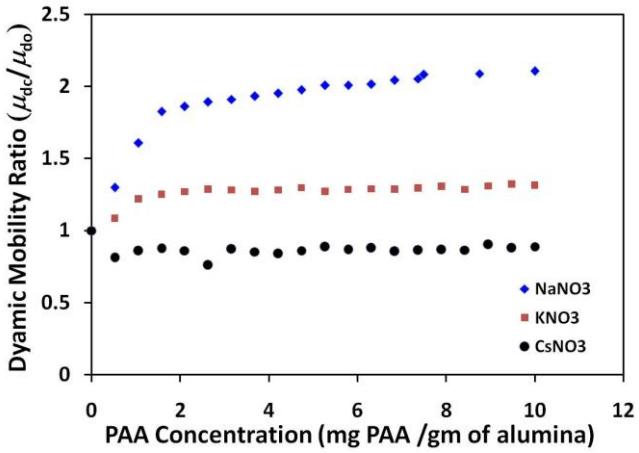

Figure 2.4 Change in dynamic electrophoretic mobility ratio (μ_{dc}/μ_{do}) of alumina particles measured by acoustic electrophoresis with addition of different poly(acrylic acid) molecular weight 200K with 1:1 electrolytes $NaNO_3$, KNO_3 and $CsNO_3$ at 0.5M concentrations; pH 12 (20 mM NaOH).

2.4 Summary

The presence of all but the lowest molecular weight PAA studied (1800) led to decreases in dynamic electrophoretic mobility at low polymer concentrations, attributable to bridging flocculation. Bridging effects increased with polymer molecular weight, and decreased with polymer concentration. Increases in background electrolyte concentration enhanced dynamic electrophoretic mobility as the polymer layers were compressed and bridging was reduced. Such enhancements were reduced as the cation was changed from K^+ to Na^+ to Cs^+. PAA chains were not completely collapsed even at 0.5 M Cs^+ concentration, and the salting-out effects are weaker than in the cases of Na^+ or K^+. At high ionic strength and strong basic environments relevant to nuclear waste slurry adsorption of PAA increases the particle surface charge thus the electrostatic repulsion forces between particles. However, changes in ionic strength (during dilution and concentration cycles) can influence PAA conformation causing aggregation due to

polymer bridging. High dosage of optimum molecular weight of PAA (10 mg/gm of alumina) can potentially avoid polymer bridging and electrosteric stabilize particles against aggregation thus reducing yield stress and viscosity.

References

1. Chun, J.; Poloski, A. P.; Hansen, E. K., Stabilization and control of rheological properties of Fe2O3/Al(OH)3 -rich colloidal slurries under high ionic strength and pH. Journal of Colloid and Interface Science 2010, 348, (1), 280-288.

2. Fleer, G. J.; Cohen Stuart, M. A.; Scheutjens, J. M. H. M.; Cosgrove, T.; Vincent, B., Polymers at interfaces. Chapman & Hall Inc.: New York, 1993.

3. Greenwood, R., Review of the measurement of zeta potentials in concentrated aqueous suspensions using electroacoustics. Advances in Colloid and Interface Science 2003, 106, 55-81.

4. Napper, D. H., Polymeric stabilization of colloidal dispersions. Academic Press Inc.: New York, 1983.

5. Palmqvista, L.; Lyckfeldta, O.; Carlströma, E.; Davoustb, P.; Kauppic, A.; Holmbergd, K., Dispersion mechanisms in aqueous alumina suspensions at high solids loadings. Colloids Surf., A 2006, 274, 100-109

6. Berg, J. C., An Introduction to Interfaces and Colloids: The Bridge to Nanoscience. World Scientific 2010; p p. 616.

7. Bulychev, N.; Dervaux, B.; Dirnberger, K.; Zubov, V.; Du Prez, F. E.; Eisenbach1, C. D., Structure of adsorption layers of amphiphilic copolymers on inorganic or organic particle surfaces. Macromolecular Chemistry and Physics 2010, 211, 971-976.

8. Carasso, M. L.; Rowlands, W. N.; O'brien, R. W., The effect of neutral polymer and nonionic surfactant adsorption on the electroacoustic signals of colloidal silica. Journal of Colloid and Interface Science 1997, 193, (2), 200-214.

9. Chibowski, S.; Wis´niewska, M., Study of electrokinetic properties and structure of adsorbed layers of polyacrylic acid and polyacrylamide at Fe2O3–polymer solution interface. Colloids and Surfaces A: Physicochem. Eng. Aspects 2002, 208, 131-145.

10. Hierrezuelo, J.; Sadeghpour, A.; Szilagyi, I.; Vaccaro, A.; Borkovec, M., Electrostatic stabilization of charged colloidal particles with adsorbed polyelectrolytes of opposite charge. Langmuir 2010, 26, (19), 15109-15111.

11. Maier, H.; Baker, J. A.; Berg, J. C., The effect of adsorbed polymers on the ESA potential of aqueous silica dispersions. Journal of Colloid and Interface Science 1987, 119, (2), 512-517.

12. Milkova, V.; Kamburova, K.; Radeva, T.; Stoimenova, M., Electrical properties of polyelectrolyte layers adsorbed on colloidal particles at different ionic strengths Langmuir 2010, 26, (18), 14488-14493.

13. Miller, N. P.; Berg, J. C., A comparison of electroacoustic and microelectrophoretic zeta potential data for titania in the absence and presence of a poly (vinyl alcohol) adlayer. Colloids and Surfaces 1991, 59, (8), 119-128.

14. Ohshima, H., Electrophoresis of Soft Particles. Advances in colloid and interface science 1995, 62 189-235.

15. Hill, R. J.; Saville, D. A.; Russel, W. B., Electrophoresis of spherical polymer-coated colloidal particles. Journal of Colloid and Interface Science 2002, 258, (1), 56-74.

16. O'Brien, R. W., The effect of an absorbed polyelectrolyte layer on the dynamic mobility of a colloidal particle. Particle and Particle Systems Characterization 2002, 19, (3), 186-194.

17. Chun, J.; Poloski, A. P.; Hansen, E. K., Stabilization and Control of Rheological Properties of Fe2O3-rich Colloidal Slurries under High Ionic Strength and pH. Jr. Colloids & Int. Sci. 2010, 348, (1), 280-288.

18. Bhosale, P. S.; Berg, J. C., Poly(acrylic acid) as a rheology modifier for dense alumina dispersions in high ionic strength environments. Colloids Surf., A: Physicochem. Eng. Aspects 2010, 362, (1-3), 71-76.

CHAPTER 3

Direct Measurements of Interparticle Interactions Using Atomic Force Microscopy

3.1 Introduction

In a dense particulate suspension, [1-4] the first step toward controlling the rheological performance of particulate suspensions is to achieve a fundamental understanding of the interparticle forces involved. This is challenging in industrially relevant complex dispersions. As pointed out previously the nuclear waste slurries are multi-component with the major solid components being aluminum hydroxides, zirconium hydroxides, ferrous hydroxides and silicon oxides residing in a strong basic environment (pH 12-13) with very high ionic strength (1.5-2 M) composed of different types of salts.[5] Table 3.1 provides a list of chemicals involved in a simulant representing nuclear waste slurry. Very few reports have studied interparticle interactions in such conditions (high salt and high pH).[6-8]

Table 3.1: Solid ingredient used to prepare 1 dm^3 of AZ-101 nuclear waste stimulant.[5]

Compounds	Formula	Mass (grams) per dm^3 of solution	Soluble fraction
Boric acid	H_3BO_3	0.073	1
Sodium chloride	NaCl	0.162	1
Sodium fluoride	NaF	0.121	1
Sodium sufate	Na_2SO_4	0.498	1
Sodium hydroxide	NaOH	10.604	1
Sodium phosphate	$Na_3PO_4.12H_2O$	7.73	1
Sodium oxalate	$Na_2C_2O_4$	0.11	1
Sodium carbonate	Na_2CO_3	5.513	1
Potassium nitrite	$NaNO_3$	0.417	1
Sodium nitrate	KNO_2	0.609	1
Sodium nitrite	$NaNO_2$	1.031	1
Iron oxide	Fe_2O_3	192.79	0
Aluminum hydroxide	$Al(OH)_3$	192.38	0
Silica	SiO_2	18.61	0.444
Zirconium hydroxide	$Zr(OH)_4$	75.66	0

Traditional colloidal theory for aqueous media predicts a destabilized colloidal system above a critical coagulation concentration (CCC) because the electric double layer surrounding the particles is collapsed, and the attractive van der Waals forces dominate interactions.[9] However, many studies have shown restabilization at high salt concentrations (above CCC), attributed to short range repulsive forces like ion specific hydration forces and interface restructuring.[7-8] This restabilization phenomenon has been reported with different surface chemistries including latex, SiO_2, alumina, and gibbsite. Since the nuclear waste slurries are also stored under high salt concentrations, what are the important interparticle interactions in these conditions? What is the interparticle bond strength or aggregate stiffness between different oxide particles under different conditions? How would the bond strength be affected on

addition of rheology modifier? We attempted to answers these questions in previous chapters using indirect measurements like those of bulk rheology, and electrokinetics. In the last 25 years, development of the surface force apparatus (SFA), and the atomic force microscope (AFM), have allowed direct measurements of surface/intermolecular forces and made tremendous impact in the field of colloidal science.[6, 10-11] Numbers of studies have used these techniques to measure surface, adhesion and frictional forces between interfaces. The main advantage, especially with AFM, is that it directly measures interparticle adhesion forces, which represent the interparticle bond strength between a desired particle and a chosen surface.

The objective of this study was to measure the interparticle interactions between various oxide surfaces using AFM at conditions similar to nuclear waste slurries and examine how polymeric rheology modifier will influence these interactions. We are especially interested in pull-off force measurements, which can be corrected to the interparticle bond strength in an aggregate. The effects of salt concentration and the addition of PAA on adhesion forces were measured for alumina/sapphire and glass particle/SiO_2 systems. The adhesion forces between SiO_2 and alumina surfaces were also measured directly in supernatant liquor from the nuclear waste simulant AZ101.

3.2 Electrostatic Repulsion Forces

The long range electrostatic interactions between alumina surfaces were measured by changing pH and salt concentration. Figure 3.1 shows the approach force-distance curves in DI water, and 0.001M KNO_3 solution at pH 6 and 11.3. In DI water, the electric double layer is very large due to low ion concentration. The increase in ionic strength to 0.001M KNO_3 reduced the double layer thickness from 80 nm to 13nm. For a single symmetrical electrolyte in water, the double layer thickness can be estimated by the Debye length (κ^{-1})

$$\kappa^{-1} = \frac{0.3041}{|z|\sqrt{C}} \tag{3.1}$$

where z is the counter ion valance and C is bulk ion concentration.[9] The measured double layer thickness of 13 nm at 0.001M KNO_3 is close to the calculated value of 10 nm. The maximum repulsive force changes from 2.5 nN to 1.5 nN because the net surface charge was shielded by adsorbed K^+ ions at the interface. The increase in pH from 6 to 11.3 enhanced the net surface charge, while ionic strength remained approximately the same. Therefore the maximum repulsion increases from 1.5 to 2nN, whereas the double layer thickness was constant. These results demonstrate the sensitivity of this technique to electrostatic interactions.

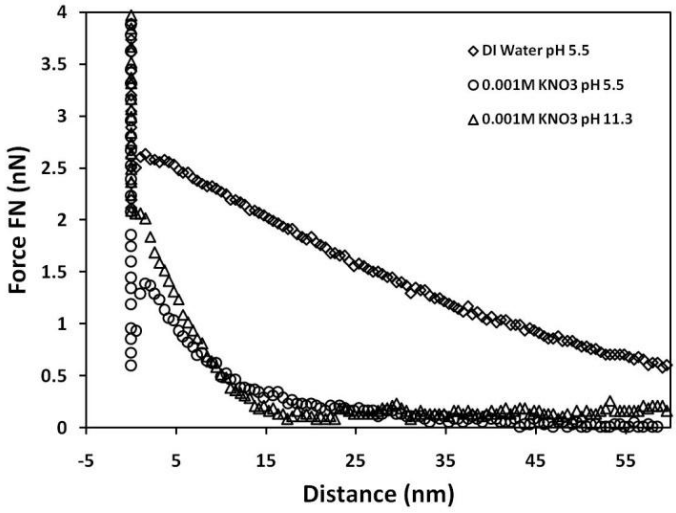

Figure 3.1: Approach force-distance curves for alumina particle against sapphire wafer in DI water, and 0.001M KNO_3 solution at pH 6 and 11.3.

3.3 Effect of Salt Concentration on Adhesion

Although electrostatic interactions are important, the adhesion forces between particles, which represent interparticle bond strength, are of more practical interest. Figure 3.2 shows the pull-off force-distance curves for an alumina particle against a sapphire surface in 0.001, 0.1 and 0.5 M KNO_3 solutions at pH 11.3. The adhesion observed is very small at 0.001 M salt concentration, due to the highly charged interfaces. At higher salt concentrations 0.1M and 0.5M, the electrostatic interactions are screened and the pull-off force increased to 0.06 $\pm$ 0.03 and 0.1 $\pm$ 0.02 mN/m respectively. An increase in the adhesion with increasing salt concentration is consistent with the literature results.[8, 10]

A complicating factor is, as is well known, that the adhesion forces vary greatly with surface roughness, measurement conditions, contact area and time. Here

large fluctuations in the measurements may have been due to surface roughness, and defects in the alumina probe particle.

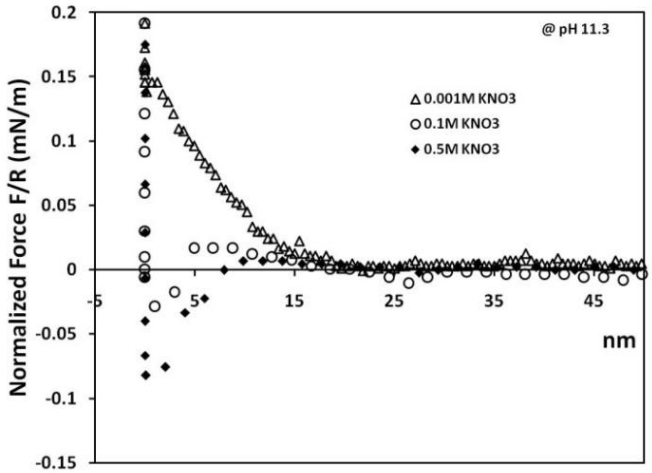

Figure 3.2: Pull-off force-distance curves for alumina particle against sapphire wafer in 0.001, 0.1 and 0.5M KNO_3 solution at pH 11.3.

3. 4 Optimum Molecular Weight

In chapter 1, it was shown that the correct choice of molecular weight of the PAA was especially important to its effectiveness as a rheology modifier: too low a value provides insufficient steric stabilization, while too high a value induces bridging. This result was also supported by direct force-distance measurements. Figure 3.3 shows the effect of PAA addition on the pull-off force-distance curves for alumina particle against sapphire surface in 0.1M KNO_3 solution at pH 11.3. Addition of low molecular weight PAA 50K leads to the formation of a steric barrier, whereas high molecular weight, PAA 450K, induces higher adhesion due polymer bridging.

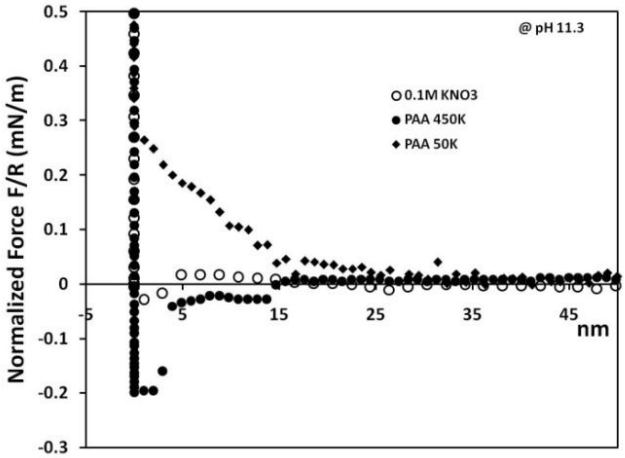

Figure 3.3: Effect of PAA 50K and 450K addition (150 ppm) to the pull-off force-distance curves for alumina particle against sapphire wafer in 0.1M KNO_3 solution at pH 11.3.

3.6 Adhesion Forces in Nuclear Waste Simulant

The pull-off forces between an alumina particle and a sapphire surface and glass particle against a SiO_2 surface were also measured directly in supernatant liquor from the nuclear waste simulant AZ101, as shown Figure 3.4. The solution chemistry of AZ101 supernatant is provided in Table 3.1. The glass particle against the SiO_2 surface system shows higher adhesion (1.25$\pm$0.27 mN/m) compared to the alumina particle against sapphire (0.1604$\pm$0.045 mN/m). However, both systems show almost no electrostatic repulsion, due to high ionic strength. Figures 3.5 a & b, show the effect of PAA 50K MW addition on the adhesion force between alumina/sapphire and glass/SiO_2 systems, respectively. Addition of PAA 50K forms a repulsive steric barrier for the both cases, consistent with the rheological studies conducted with PAA and AZ 101 slurry.[5] The interesting result here is the formation of a steric barrier with glass particle against SiO_2 surface.

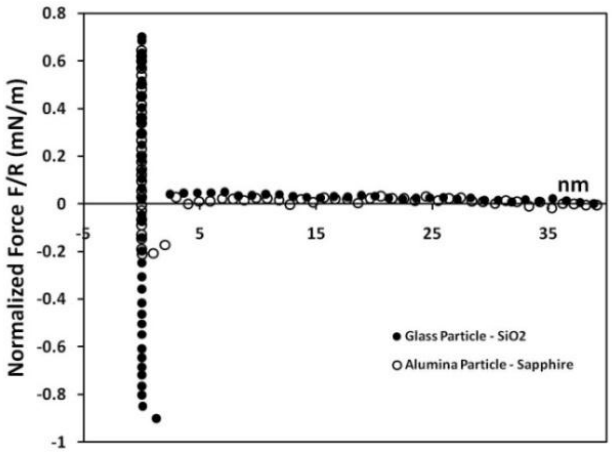

Figure 3.4: Pull-off force-distance curves for alumina particle against sapphire surface in supernatant of waste simulant AZ 101.

Negatively charged PAA can adsorb onto the negatively charged metal oxide and hydroxide surfaces (Al_2O_3, Fe_2O_3, ZrO_2 and TiO_2) at high pH (i.e. pH > 9) through hydrogen bonding between the carboxylic acid group ($–COO^-$) of the PAA and the neutral Me-OH on the metal oxide surface.[13-14] However, studies have shown that in such conditions PAA does not adsorb onto the silica surface in the presence of high monovalent cations. The force-distance curves on the other hand clearly show a steric barrier formed by PAA adsorption on silica surfaces. The PAA adsorption onto the glass and SiO_2 surfaces was evidently introduced due to the presence of multivalent ions in the solution. Berg et al.[15] and Abraham et al.[16] have identified that the presence of divalent ions (Ca^{2+}, Mg^{2+} and Ba^{2+}) initiates PAA adsorption onto mica surfaces.

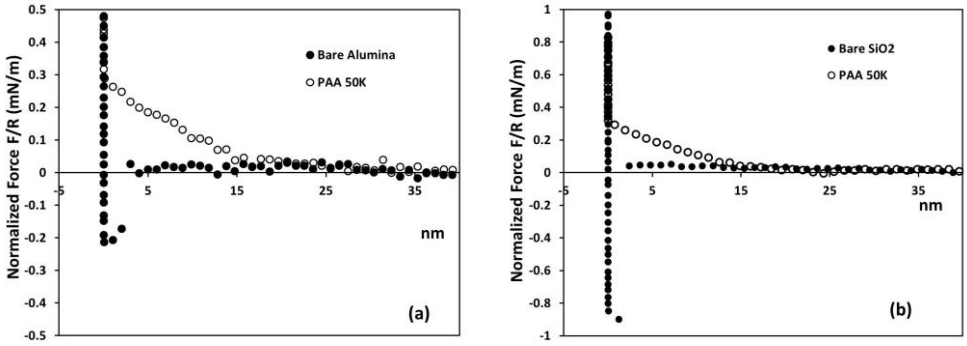

Figure 3.5: Effect of PAA 50K addition (150 ppm) to the pull-off force-distance curves for a) alumina particle against sapphire surface b) glass particle against silicon surface in supernatant of waste simulant AZ 101.

3.7 Summary

The interparticle interaction forces were directly measured using atomic force microscopy in condition similar to the nuclear waste slurries. The long range electrostatic repulsion between alumina and silica particles is screened and the adhesion force is strengthened with increasing ionic strength (0.1 to 0.5 M of K^+). In the nuclear waste simulant AZ 101 the net adhesion force was higher for silica surfaces compared to alumina surfaces. The addition of optimum molecular weight of poly (acrylic acid) reduced the particle adhesion due to electrosteric repulsion forces. It was also shown that in the nuclear waste simulant poly (acrylic acid) adsorbs on silica surfaces due to presence of divalent ions. Poly (acrylic acid) can adsorb on the different oxide particles (Al_2O_3, Fe_2O_3, ZrO_2, TiO_2 and SiO_2) in the nuclear waste slurry and reduce particle adhesion.

References

1. Lu, P. J.; Zaccarelli, E.; Ciulla, F.; Schofield, A. B.; Sciortino, F.; Weitz, D. A., Gelation of particles with short range attraction. *Nature* **2008,** 453, 499-503

2. Pickrahn, K.; Rajaram, B.; Mohraz, A., Relationship between microstructure, dynamics, and rheology in polymer-bridging colloidal gels. *Langmuir* **2009,** 26, (4), 2392–2400.

3. Wyss, H. M.; Tervoort, E. V.; Gauckler, L. J., Mechanics and Microstructures of Concentrated Particel Gels. *J. Am. Ceram. Soc.* **2005,** 88, (9), 2337-2348.

4. Mewis, J.; Wagner, N. J., Current trends in suspension rheology. *J. Non-Newtonian Fluid mech.* **2009,** 157, 147-150.

5. Chun, J.; Poloski, A. P.; Hansen, E. K., Stabilization and control of rheological properties of Fe_2O_3/$Al(OH)_3$ -rich colloidal slurries under high ionic strength and pH. *Journal of Colloid and Interface Science* **2010,** 348, (1), 280-288.

6. Fielden, M. L.; Hayes, R. A.; Ralston, J., Oscillatory and ion-correlation forces observed in direct force measurments between silica in concentrated $CaCl_2$ solutions. *Phys. Chem. Chem. Phys* **2000,** 2, 2623-2628.

7. Stenkamp, V. S.; McGuiggan, P.; Berg, J. C., Restabilization of Electrosterically Stabilized Colloids in High Salt Media. *Langmuir* **2001,** 17, (3), 637-651.

8. Yilmaza, H.; Satoa, K.; Wataria, K., AFM interaction study of α-alumina particle and c-sapphire surfaces at high-ionic-strength electrolyte solutions. *Jr. Colloids & Int. Sci.* **2007,** 307, (1), 116-123.

9. Berg, J. C., *An Introduction to Interfaces and Colloids: The Bridge to Nanoscience*. World Scientific 2010; p p. 616.

10. Vakarelski, I. U.; Higashitani, K., Dynamic Features of Short-Range Interaction Force and Adhesion in Solution. *Jr. Colloids & Int. Sci.* **2001,** 242, 110-120.

11. Ralston, J.; Larson, I.; Rutland, M. W.; Feiler, A. A.; Kleijin, M., Atomic force miscroscope and direct surface force measurements. *Pure Appl. Chem.* **2005,** 77, (12), 2149-2170.

12. Cleveland, J. P.; Manne, S.; Bocek, D.; Hansma, P. K., A nondestructive method for determining the spring constant of cantilevers for scanning force microscopy. *Rev. Sci. Instrum.* **1993,** 64, (2), 403-405.

13. Bhosale, P. S.; Chun, J.; Berg, J. C., Electrophoretic mobility of poly(acrylic acid)-coated alumina particles. *Jr. Colloids & Int. Sci.* **2011,** 258, 123-128.

14. Chibowski, S.; Wis´niewska, M., Study of electrokinetic properties and structure of adsorbed layers of polyacrylic acid and polyacrylamide at Fe_2O_3–polymer solution interface. *Colloids and Surfaces A: Physicochem. Eng. Aspects* **2002,** 208, 131-145.

15. Berg, J. M.; Claesson, P. M.; Neuman, R. D., Interactions between Mica Surfaces in Sodium Polyacrylate Solutions Containing Calcium Ions. *Jr. Colloids & Int. Sci.* **1993,** 161, (1), 182-189

16. Abraham, T.; Kumpulainen, A.; Xu, Z.; Rutland, M.; Claesson, P. M.; Masliyah, J., Polyelectrolyte-Mediated Interaction between Similarly Charged

Surfaces: Role of Divalent Counter Ions in Tuning Surface Forces. *Langmuir* **2001,** 17, 8321-8327.

CHAPTER 4

Polymer Bridge Formation and Disruption Dynamics and its Effect on the Bulk Rheology of Suspensions

4.1 Introduction

Interparticle interactions especially particle adhesion is dynamic in nature[1-5] and has practical implications for dense slurry transport. Particles can accumulate and aggregate and sinter over time in dead zones (bends, elbows and pumps etc.) of nuclear waste transport systems, and negatively impact the flow rate. It is very difficult to remove sintered bocks in the dead zones. This is highly undesirable. In this chapter the focus is on the dynamics of particle contact. Previous reports have investigated bare particle adhesion dynamics and shown that the dynamics of particle adhesion plays a central role in slurry rheology.[3,5-9] AFM measurements by Vakarelski et al.[5] reveled increased adhesion between SiO_2 and mica surfaces with contact time due to the disruption of the hydration layer between the two surfaces. Optical tweezer studies by Meng et al.[3] also showed increased adhesion between polystyrene particles with time. The contact area between the soft polystyrene particles increased with time leading to higher adhesion. Diffusing wave spectroscopy and bulk rheological measurements have shown that this increased particle adhesion leads to a higher

elastic modulus of the suspension.[8] However, very few studies[4, 10-11] have investigated particle adhesion dynamics in the presence of polymers or surfactants, motivating the characterization of particle adhesion/contact dynamics with and without polymeric rheology modifiers. The consequences of this adhesion dynamics for bulk rheological performance are also unexplored.

The addition of polymeric modifiers can induce attractive forces between colloidal particles by bridging and depletion flocculation.[12] Both adhesion mechanisms are dynamic in nature. While theoretical studies of polymer adsorption and desorption are focused primarily on equilibrium, such conditions may not prevail in practice.[13] Recently, Sprakel et al.[4] addressed this issue by measuring the kinetics of polymer bridging and disruption experimentally using atomic force microscopy (AFM) for the case of polyethylene oxide MW 14-20 $x10^3$ g/mol adsorbed on SiO_2 surfaces. It was shown that the adhesion force increased with contact time as the number of polymer bridges increased.

However, the above study left unanswered a number of questions, e.g. 1) If the polymer bridge is broken, does the polymer desorb from the surface or is the polymer backbone broken? 2) When contact is re-established, what is the strength of the reformed bridge? 3) If polymer chains scission is possible, how many times can such contact be re-established? 4) What are the consequences of repeated contact and disruption on bulk rheology? To address these questions dynamics of polymer bridge formation and disruption was investigated for a model system of silica particle suspension flocculated by polyethylene oxide (PEO). The adhesion dynamics was

studied at microscale using AFM pull-off force measurements for a spherical silica colloidal probe against a flat silica surface in the presence of an aqueous solution of polyethylene oxide MW 10^5 g/mol. We specially focused on repeated disruption and establishment of polymer bridges under conditions believed to be relevant to practical flow situations. The consequences of this adhesion dynamics for the bulk rheological performance were studied by macroscopic oscillatory rheology measurements conducted on dense aqueous silica slurries in the presence of the same polymer. The slurries were subjected to various levels of repeated mixing and rest time to investigate the correlation, if any, between the macroscopic behavior and microscopic dynamics of bridge formation and disruption.

4.2 Polymer Bridge Disruption

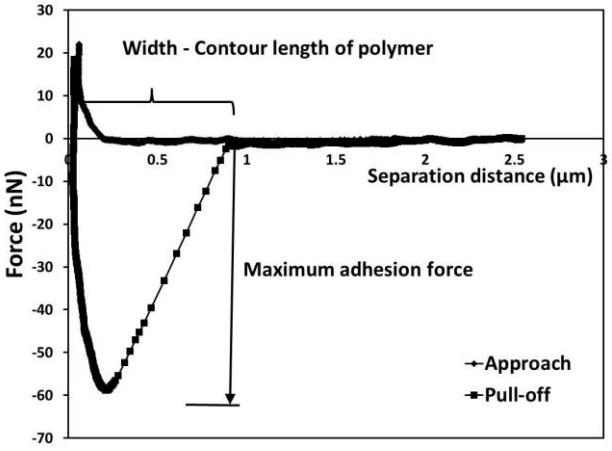

Figure 4.1: AFM approach and pull-off force vs. distance curves obtained for a spherical silica colloidal probe against SiO_2 substrate in 0.02 g/L solution of PEO MW 10^5 g/mol in water (0.01M KNO_3). Probe velocity 300 nm/s.

Figure 4.1 shows the approach and pull-off force distance curves obtained by an AFM with a spherical silica probe particle against a SiO_2 substrate in 0.02 g/L solution of PEO MW 10^5 g/mol in DI water (0.01 M KNO_3). On approach toward the substrate, the silica probe experienced a steric repulsion, whereas upon pull-off, a strong adhesion force was measured as the PEO chains bridged the two surfaces. A gradual decrease in adhesion force shows a consecutive breaking of polymer bridges. As the two surfaces are separated, the polymer backbone is stretched, and bridges are broken at different separation distances. The full width of the pull-off curve should represent the contour length of the adsorbed polymer. The calculated contour length of PEO MW 10^5 g/mol is 900 nm, assuming a Kuhn length 0.9 nm and 1000 segments.[4] This is comparable to the width of the pull-off curve, 883 nm. The maximum adhesion force can be correlated to the number of bridges formed between the two surfaces if the molecular weight and number of polymer segments adsorbed on the surface are known.[4] Similar to the previously reported results for the high molecular weight PEO used (MW 100 x 10^3 g/mol) the maximum adhesion forces increased as the surface delay time increased from 0 to 10 seconds due to increase in the number bridges formed between two surfaces. Results are shown in our recent work.[14]

4.3 Repeated Polymer Bridge Disruption

To study the effect of repeated disruption and establishment of bridges, the pull-off force measurements were carried out repeatedly with a constant probe velocity

(300 nm/s), a constant approach time (6.6s) to the surface and a constant surface delay time before disruption. Surface delay time is the amount of time the colloidal probe was in contact with the surface before pull-off was initiated. Figure 4.2 shows the maximum adhesion force plotted against the number of repeated contacts (contact number) at varying surface delay times.

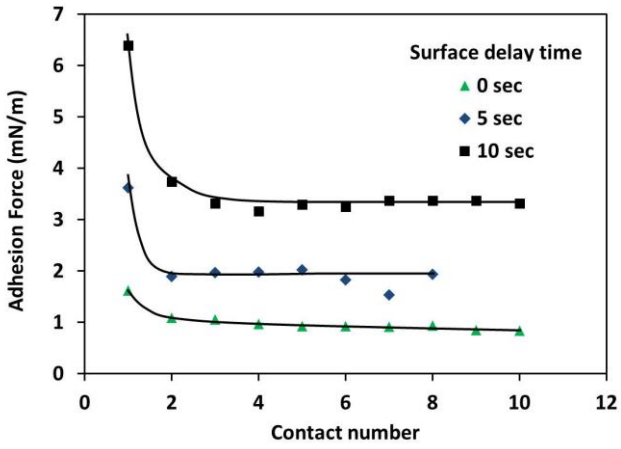

Figure 4.2: Maximum pull-off force measured on repeated contact with varying surface delay times (probe velocity 300 nm/s). The lines drawn are guide to the eye.

After disruption of the first contact, a significant decrease in maximum adhesion force was observed, followed by very small decreases in adhesion after the third contact. The net decrease in adhesion after the first contact was higher for higher contact times. This decrease in adhesion was probably caused by chain scission during contact disruption. Figure 4.3 shows pull-off force vs. distance curves for the first and fifth contacts at surface delay times of five seconds. A decrease in the width of the pull-off curve suggests lower contour lengths of the polymer fragments on the surface. During contact disruption, the polymer chains are stretched and subjected to elongation stresses which cause chain scission. This chain scission is similar to the mastication of

polymer chains in elongation and shear flows which was first report by Staudinger in early 1930's.[15-17] In dilute polymer solutions above a critical flow velocity gradient the polymer becomes partially uncoiled and ruptures.[18] Midsection cleavage theory showed that the central bond in the polymer coil experiences the highest mechanical stress and has the highest probability to break.[19-22] When two surfaces are pushed together the polymer chain adsorbs in the spaces between the polymers. After the chain scission, the smaller polymer fragments left on the surface increase the polymer segment density. These fragmented polymer chains form weaker contacts upon second and third repeats. The scission is dominant with long polymer chains.[18]After the third contact, further decreases in adhesion were minimal, suggesting that the polymer scission was limited after the first disruption.

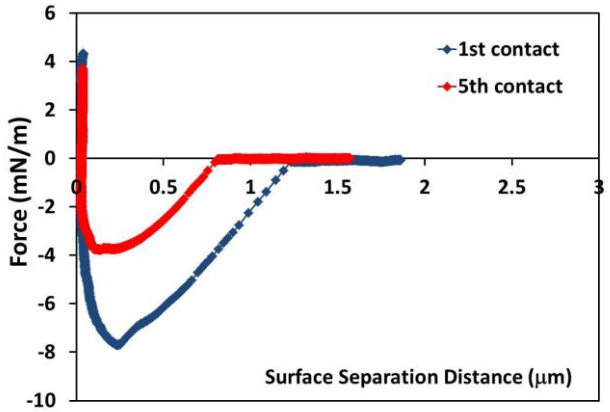

Figure 4.3: Pull-off force vs. distance curves at the first and fifth contacts for PEO 10^5 g/mol adsorbed on silica surfaces (probe velocity of 300 nm/s and 5s surface delay time).

4.4 Effect on Bulk Rheology

The consequences of the adhesion dynamics on the bulk properties of flocculated silica particle suspensions was studied using oscillatory rheometry. Figure 4.4 shows (a) frequency and (b) amplitude sweeps for 62 wt% silica particle (1 μm) suspension with PEO MW 4 x 10^6 g/mol in DI water (0.01 KNO_3). The frequency sweep (0.01% strain) showed a linear viscoelastic response up to 100 Hz, and the amplitude sweep showed a yield stress at 100 Pa. The yield stress point can be recognized as the stress at which the loss modulus, which represents viscous properties, surpasses the storage modulus, which represents the elastic properties of the suspension. At the yield stress, interparticle bonds are broken leading to a viscoplastic flow.[23] The storage modulus measured below the yield stress can be correlated directly to interparticle bond strength.[24]

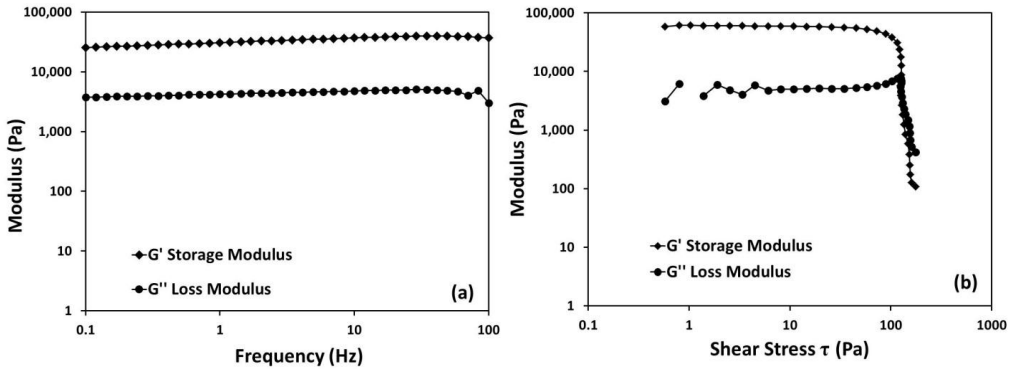

Figure 4.4: Frequency (a) and amplitude (b) sweep for 62 wt% silica particle (1 μm) dispersion bridge flocculated with 2.5 mg/gm of PEO MW 4 x 10^6 g/mol in DI water (10^{-2} M KNO_3).

To study the effect of repeated disruption and re-establishment of particle contact on the bulk rheological properties, repeated amplitude sweep tests were

performed. In each test the applied shear was increased above the yield stress to breakdown the particle network. In figure 4.5, the change in the plateau storage modulus is plotted vs. repeat test number. Similar to the colloidal probe AFM measurements (figure 4.2), on repeated break down of the flocculated suspension, a large drop followed by a gradual decrease in the storage modulus was observed. The same trend was observed for the case of a 1000s delay time between repeat tests, but the net storage modulus was higher, corresponding to stronger adhesion between particles. The delay time between tests allows the interparticle bond to strengthen, as the number of bridges formed between particles increases with time. After the third repeat the net decrease in modulus was higher compared to the decrease in adhesion force measured by AFM. The high molecular weight PEO (4 x10^6 g/mol) used in the bulk rheology measurements can undergo chain scission multiple times compared to the PEO MW 10^5 g/mol used in AFM measurements. This additional chain scission gradually reduces particle adhesion after the third repeat.

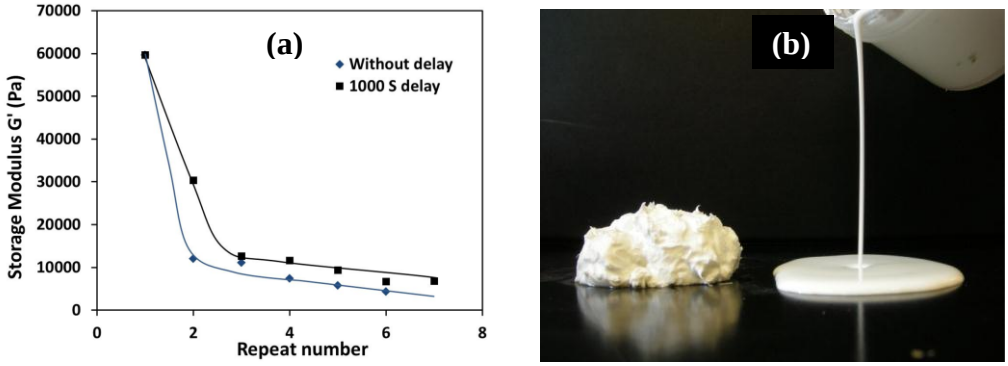

Figure 4.5: (a) Change in plateau storage modulus at low shear stress (0.1-1 Pa) with repeated amplitude sweep for 62 wt% silica particle (1 μm) dispersion with 2.5 mg/gm PEO MW 4 x 10^6 g/mol in DI water (10^{-2} M KNO_3). Lines are to guide the eye and not actual fit to the data. (b) Silica particle (1 μm) suspension bridge flocculated by PEO MW 4 x 10^6 g/mol before and after the mixing in SpeedMixer™ for 6 min at 3300 rpm.

To further study the hypothesis of chain scission during polymer bridge disruption, we subjected the flocculated silica particle suspensions to very high shear rates for long periods (6 min at 3300 rpm), in the SpeedMixer™. When subjected to such high shear conditions, particles go through multiple cycles of contact and disruption during which chain scission should be amplified. Figure 4.6 (b) shows a flocculated silica particle dispersion before (left) and after (right) shear mixing. The flocculated particle network broke down irreversibly, and free flowing slurry was obtained. Amplified chain scission results in fragmented polymer chains that are unable to bridge-flocculate the particles, further corroborating the of microscale indications of chain scission obtained by AFM measurements.

4.5 Summary

The dynamics of polymer bridge formation and disruption was measured using colloidal probe microscopy for the case of polyethylene oxide adsorbed on silica surfaces. Adhesion between bridge-flocculated particles increases with contact time as the number of polymer bridges formed increases with time. Upon disruption and re-establishment of the contact, a significant decrease in maximum adhesion was observed. This was attributed to chain scission during pull-off, leaving fragments of lower molecular weight polymer on the surfaces. These smaller fragments then form weaker adhesion on the second and third contacts. After the third contact, very small

further decreases, in adhesion were observed; indicating chain scission reduced significantly after the first few contacts. The net decrease in adhesion was higher for higher contact times.

The consequences of the microscale dynamics for the macroscale properties i.e. the storage and loss moduli of the bridge-flocculated silica suspension was studied using oscillatory rheometry. Similar to the colloidal probe AFM measurements, on repeated breakdown of a flocculated silica particle suspension, a large drop followed by gradual decrease in the storage modulus was observed. When the flocculated suspension was subjected to the high shear for long periods (3-6 min), the gel network broke down irreversibly, and free flowing slurry was obtained, further supporting the hypothesis of chain scission of the polymer as the bridged contacts are disrupted.

References

1. Frens, G., Interacting Particles in Contact. *Faraday Discuss. Chem. Soc.* **1990,** 90, 143-151.

2. Manley, S.; Davidovich, B.; Davies, N. R.; Cipelletti, L.; Bailey, A. E.; Christianson, R. J.; Bowen, I. J.; Eggers, J.; Kurta, C.; Lorik, T.; Weitz, D. A., *Phys. Rev. Lett.* **2005,** 95, 048302.

3. Meng, B.; Wu, J.; Li, Y.; Lou, L., Aging process of the bond between colloidal particles. *Colloids Surf., A: Physicochem. Eng. Aspects* **2008,** 322, 253-255.

4. Sprakel, J.; Bartscherer, E.; Hoffmann, G.; Stuart, M. A. C.; Gucht, J. v. d., Dynamics of polymer bridge formation and disruption. *Phys. Rev. E* **2008,** 78, 0402802.

5. Vakarelski, I. U.; Higashitani, K., Dynamic Features of Short-Range Interaction Force and Adhesion in Solution. *Jr. Colloids & Int. Sci.* **2001,** 242, 110-120.

6. Pantina, J. P.; Furst, E. M., Elasticity and critical bending moment of model colloidal aggergates. *Phys. Rev. Lett.* **2005,** 94, 138301.

7. Pantina, J. P.; Furst, E. M., Colloidal aggergate micromechanics in the presence of divalent ions. *Langmuir* **2006,** 22, (12), 5282-5288.

8. Manley, S.; Davidovitch, B.; Davies, N. R.; Cipelletti, L.; Bailey, A. E.; Christianson, R. J.; Gasser, U.; Prasad, V.; Segre, P. N.; Doherty, M. P.; Sankaran, S.; Jankovsky, A. L.; Shiley, B.; Bowen, J.; Eggers, J.; Kurta, C.; Lorik, T.; Weitz, D. A., Time-Dependent Strength of Colloidal Gels. *Phys. Rev. Lett.* **2005,** 95, (4), 048302.

9. Shahin, A.; Joshi, Y. M., Hyper-Aging Dynamics of Nanoclay Suspension. *Langmuir* **2012,** 28, (13), 5826-5833.

10. Kamibayashi, M.; Ogura, H.; Otsubo, Y., Rheology of complex suspensions flocculated by associating polymers. *Journal of Rheology* **2006,** 50, (6), 1009-1023.

11. Braithwaite, G. J. C.; Howe, A.; Luckham, P. F., Interactions between Poly(ethylene oxide) Layers Adsorbed to Glass Surfaces Probed by Using a Modified Atomic Force Microscope. *Langmuir* **1996,** 12, (17), 4224-4237.

12. Napper, D. H., *Polymeric stabilization of colloidal dispersions*. Academic Press Inc.: New York, 1983.

13. Fleer, G. J.; Cohen Stuart, M. A.; Scheutjens, J. M. H. M.; Cosgrove, T.; Vincent, B., *Polymers at interfaces*. Chapman & Hall Inc.: New York, 1993.

14. Bhosale, P. S.; Berg, J. C., The dynamics of polymer bridge formation and disruption and its effect on the bulk rheology of suspensions. *Langmuir* **2012,** in press.

15. Staudinger, H.; Leupold, E. O., Isoprene and rubber. XVIII. Studies of the viscosity of balata. *Berichte der Deutschen Chemischen Gesellschaft [Abteilung] B: Abhandlungen* **1930,** 63B, 730-733.

16. Staudinger, H., Isoprene and rubber. XX. Colloidal nature of rubber, gutta-percha and balata. *Berichte der Deutschen Chemischen Gesellschaft [Abteilung] B: Abhandlungen* **1930,** 63B, 921-934.

17. Staudinger, H.; Heuer, W., Highly polymerized compounds. XCIII. The breaking up of the molecular fibers of the polystyrenes *Berichte der Deutschen Chemischen Gesellschaft [Abteilung] B: Abhandlungen* **1934,** 67B, 1159-1164.

18. Sim, H. G.; Khomami, B.; Sureshkumar, R., Flow--induced chain scission in dilute polymer solutions: Algorithm development and results for scission dynamics in elongational flow. *Journal of Rheology* **2007,** 51, (6), 1223-1251.

19. Buchholz, B. A.; Zahn, J. M.; Kenward, M.; Slater, G. W.; Barron, A. E., Flow-induced chain scission as a physical route to narrowly distributed, high molar mass polymers. *Polymer* **2004,** 45, (4), 1223-1234.

20. Nguyen, T. Q., Dynamics of Flexible Polymer Chains in Elongational Flow *CHIMIA* **2001,** 55, (3), 147-154.

21. Nguyen, T. Q.; Kausch, H. H., Effects of solvent viscosity on polystyrene degradation in transient elongational flow. *Macromolecules* **1990,** 23, (24), 5137-5145.

22. Kauzmann, W.; Eyring, H., The Viscous Flow of Large Molecules. *Journal of the American Chemical Society* **1940,** 62, (11), 3113-3125.

23. Berg, J. C., *An Introduction to Interfaces and Colloids: The Bridge to Nanoscience*. World Scientific 2010; p p. 616.

24. Mewis, J.; Wagner, N. J., *Colloidal suspension rheology*. Cambridge University Press: Cambridge; New York, 2012.

CHAPTER 5

Acoustic Spectroscopy & Electroacoustics of Particles Dispersed in Polymer Gel

5.1 Introduction

Particles dispersed in a gel system (gel-trapped colloids[1] or hydrogel nanocomposites[2]) are widely used for a number of applications including separations[2-3] (gel electrophoresis), growth of high quality crystals/particles, for suspending particles[4] (in the food and pharmaceutical industries) and drug delivery.[5] However, techniques for characterizing gel-trapped or gel-suspended particles size and dynamics remain rather limited due to primarily two problems 1) non-homogeneity in the gel matrix and 2) optical contrast between particles and the gel medium.[5] Conventional light scattering requires special conditions, such as low particle concentration and the use of transparent gels (matching refractive index of polymer and liquid) to characterize the particles. Electroacoustics and acoustic spectroscopy are novel, and noninvasive techniques used for particle surface charge and particle size distribution (PSD) determinations in dense dispersions, respectively.[6-7] Acoustic techniques can potentially overcome the limitations of the conventional techniques and provide simple alternative for characterization of the opaque colloidal dispersions in polymer

gels.[7-9] Theoretical models have suggested that in particular, electroacoustic might be used to characterize the electrokinetic properties of particles in viscoelastic media.[2, 10-11] However, to the best of our knowledge, there have been no experimental studies investigating electroacoustics or acoustic attenuation of gel-trapped particles. As a side project we have attempted to expand acoustic techniques for characterization of particles dispersed in polymer gel.

5.2 Acoustic Spectroscopy

In acoustic spectroscopy a monochromatic longitudinal ultrasound wave (1 to 100MHz) is passed through a colloidal dispersion, and the loss of amplitude (attenuation) and the speed of sound are measured to predict the PSD. Fundamental studies in the 1940's[12-13] and 50's[14-15] and in particular those by Allegra et al.[16] in the 1970's correlated the attenuation of the signal (α) by viscous losses to the particle radius (R), density contrast and the frequency (ω). For a model system of monodispersed submicron spherical particles dispersed in a Newtonian fluid at low-to-intermediate frequencies:[8]

$$\frac{\alpha}{\phi} = \frac{1}{9}\omega^2 R^2 \frac{\rho}{c\mu}\left(\frac{\rho_p}{\rho} - 1\right)^2 , \qquad (5.1)$$

where ϕ is volume fraction of the particles, c is speed of sound, μ is the viscosity of the medium, and ρ and ρ_p are the medium and particle density, respectively. In the 1980's[17] and 90's Dukhin and Goetz[6-7] and others[18] developed the models further

using numerical methods to characterize dispersions with polydispersity, strong interparticle interactions and multicomponent systems. A typical modern acoustic spectroscopy instrument yields the attenuation vs. frequency curve for the system, which is then fitted by the relevant model considering different types of losses and scattering mechanisms to predict the particle size distribution.

Here we have applied acoustic spectroscopy to characterize particle size distributions in hydroxylpropyl cellulose (HPC) gel systems containing silica nanoparticles. HPC is widely used in various food and pharmaceutical products, for example, as a binder in tablets,[19] a thickener or stabilizer in food products, and as a rheology modifier in artificial tears.[20] As the particle motion with respect to the medium is very small in acoustic testing (at maximum attenuation, it is comparable to the particle size), we speculate that when the particles are smaller than the hydrodynamic gel mesh size, χ_e, as suggested in Figure 5.1, their mobility should be identical to that found in pure solvent. It may then be used to predict the hydrodynamic size of the particles or the PSD in the gel medium using current acoustic attenuation theory derived for Newtonian media. The objective of acoustic spectroscopy studies was to experimentally probed this hypothesis and explore its limits. The polymer mesh size relative to the particle size is systematically varied to explore the effects on particle mobility.

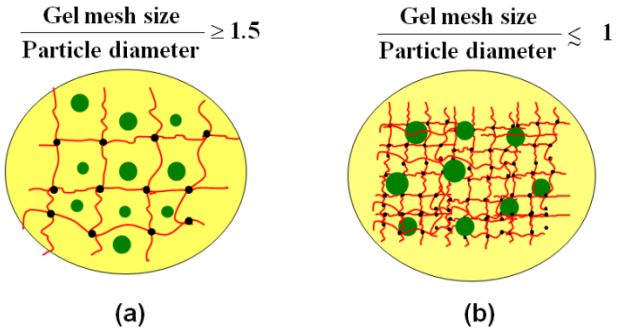

Figure 5.1: Particles confined in a polymer gel system a) particles smaller than the mesh size b) particles larger than the mesh size.

In Figure 5.2 the attenuation curve for the 29.6 nm silica particles dispersed in 0.5 wt% HPC gel (χ_e = 57.6 nm) and water are plotted together with the background curves for pure water and gel in the absence of particles. The inset in Figure 5.2 shows the particle size distribution with a mean diameter of 30 ± 1 nm as calculated by the instrument software based on the model developed by Dukhin and Goetz.[6-7] The indicated PSD was found to be identical to that in pure water provided that the hydrodynamic particle diameter, as given by dynamic light scattering, was less than the hydrodynamic mesh size of the gel, as given by simple rubber elasticity theory, (mesh size/particle size $\gtrsim$ 1.5). The same results were obtained at particle loadings of up to at least 15 wt%, beyond which measurements could not be made for the systems studied.

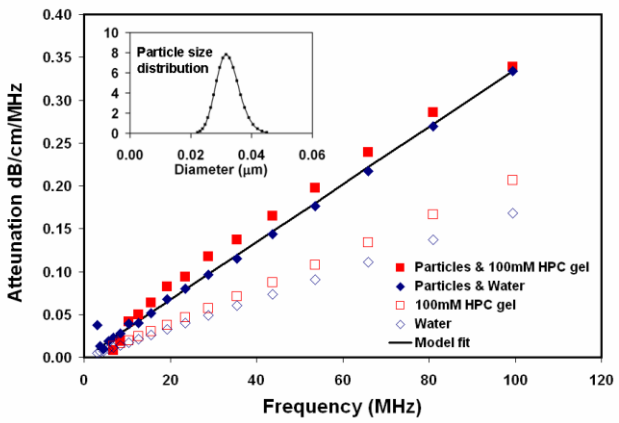

Figure 5.2: Acoustic attenuation at various frequencies through 0.5 wt% HPC gel (100 mM DVS, i.e., χ_e=57.6 nm) and water loaded with 6 wt% silica nanoparticles (26.9 nm). Experimental data were fitted using the Allegra et al.[16] model (Eq. 5.1), plotted as a line, to predict particle size of 30 nm (inset). Background attenuation signals from water and the HPC gel are represented by the empty symbols.

To explore the case of particles trapped in the gel, i.e., for mesh sizes smaller than the particle size we systematically varied the cross linker DVS concentration from 70mM to 400mM producing mesh sizes in 0.5wt% HPC gel as summarized in Table 3.1: 70.8 nm, 56.8nm, 45nm and 19.1nm at 75mM, 100mM, 200mM and 400mM DVS, respectively. Figure 5.3 shows the corresponding attenuation curves. The particle mean diameters as computed by acoustic attenuation theory are tabulated in Table 5.1, which shows that for mesh sizes larger than the particle size (29.6 nm), the attenuation spectra were almost identical to those of silica particles dispersed in water. However, at 400 mM of DVS (mesh size 19.1 nm) the indicated diameter was 71 nm, much larger than the actual size. Particles in such a gel are trapped, as suggested in Figure 5.1(b). If the particles are larger than the mesh size, a viscoelastic response from the gel matrix is observed which cannot be interpreted to yield particle size using the existing theoretical framework. Current models would need to be extended in order to

account for the elastic response of the medium and to accurately predict the PSD for gel-trapped colloids. If such models are successfully developed the acoustic attenuation can be used to probe visco-elastic properties (microrheology) of the polymer gel matrix at MHz frequencies.

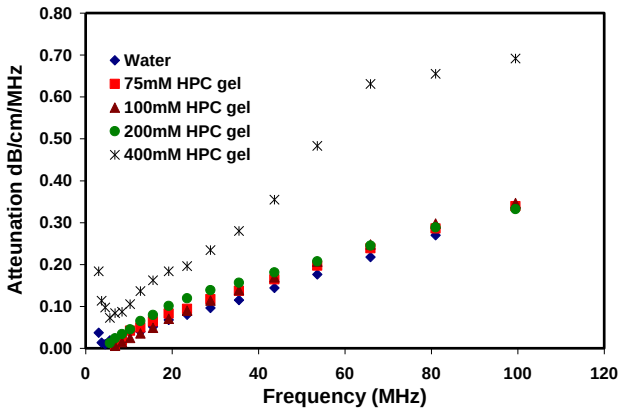

Figure 5.3: Acoustic attenuation at various frequencies through 0.5 wt% HPC gel with different cross linker concentrations (75, 100, 200 and 400 mM DVS) in comparison with particles in water. All the dispersions are loaded with 6 wt% silica nanoparticles (26.9 nm).

Table 5.1. Mean particle diameters as inferred from acoustic attenuation data for 0.5 wt% HPC gel with different cross linker concentration. Gel loaded with 6 wt% of 29.6 nm silica nanoparticles particles.

Cross Linker conc. (mM)	Mesh Size (nm)	Acoustic Attenuation Measurements		Mean diam. by light scattering (nm)
		Indicated diam. in water (nm)	Indicated diam. in gel (nm)	
75	70.8	30±1	29.1±1.2	29.6±1.8
100	56.8	30±1	29.7±1.5	29.6±1.8
200	45	30±1	31.7±1.1	29.6±1.8
400	19.1	30±1	71±0.9	29.6±1.8

5.3 Electroacoustics

In electroacoustics, the colloidal particles are subjected to oscillatory motion using longitudinal ultrasound waves (1-20MHz) which produce an alternating polarization of the electric double layer around the particles. The alternating current (colloid vibration current, CVI) or voltage (ultrasonic vibration potential, UVP) generated by the double layer polarization is used to determine dynamic electrophoretic mobility, μ_d, analogous to the classical electrophoretic mobility, u_E. The measured CVI yields the dynamic electrophoretic mobility (μ_d) of the individual particles in accord with

$$\mathrm{CVI} = A\phi\mu_d \frac{\rho_p - \rho_m}{\rho_m}, \tag{5.2}$$

where ϕ is particle volume fraction, ρ_p and ρ_m are the densities of the particles and the medium, respectively, and A is an instrument constant.

The dynamic mobility, μ_d, may be used to calculate the electrical properties of the particles such as zeta potential or surface charge density.[8] In electroacoustics the oscillatory motion of the particle is very small compared to its diameter.[17, 21,10] Therefore, one would expect that the dynamic electrophoretic mobility of the particles suspended in the gel would be the same as in the background medium if the particles are smaller than gel mesh size, but the case of gel-trapped particles may be more complicated. Recently, Wang and Hill[10] proposed a model for the dynamic electrophoretic mobility of gel-trapped particles at frequencies up to 1GHz.

Specifically, it was suggested that at high enough frequencies (MHz), and shear moduli less than approximately 10 kPa, the dynamic electrophoretic mobility of the particles should be independent of the elasticity of the gel medium (presumably whether or not the particles are trapped). For higher gel moduli, μ_d was predicted to drop. The electroacoustic study was aimed at investigating the electrokinetic behavior of particles in viscoelastic gel media, with the particle size either less than or greater than the gel mesh size, using commercial instrumentation. Specifically, it seeks: 1) to examine the hypothesis that if the particles are smaller than the gel mesh size, particle dynamic electrophoretic mobility (as measured in terms of the colloid vibration current, CVI) is the same as in the background medium, and 2) to investigate, for the case of gel-trapped particles, the dependence, if any, of the dynamic mobility μ_d on the gel storage modulus, *G*', for a given particle size, and on the particle size for a gel of given *G*'.

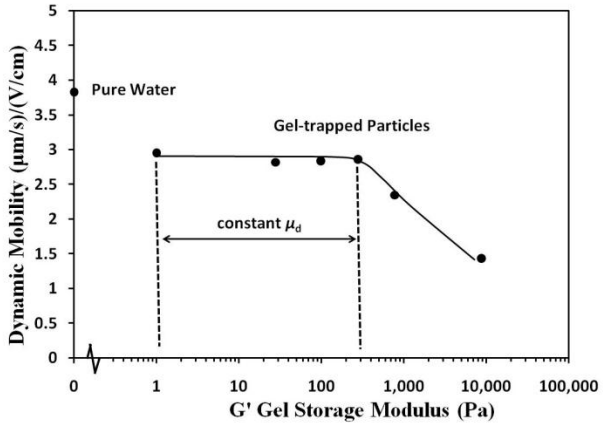

Figure 5.4: Dynamic electrophoretic mobility (μ_d) of silica particles (30 nm) trapped in a polyacrylamide gel with different storage modulus (*G*'). All the mobility's were measured at 80 min. The *G*' increased from 1 to 300 Pa (increased crosslink density) by changing monomer to crosslinker ratio from 100:1 to 10:1 at 3 wt% monomer concentration. *G*' was further increased up to 871 and 8690 Pa by the increasing monomer concentration to 5 and 10 wt% respectively at 60:1 monomer-to-crosslinker ratio.

For the case of particle size smaller than the gel mesh size, the dispersion studied was 30 nm silica particles at a concentration 9 wt% suspended in 0.5 wt% HPC hydrogels of 56.7 nm mesh size.[21] The dynamic electrophoretic mobility μ_d for the particles was found to be the same as in water. Therefore in such systems electroacoustics can be used directly to measure the electrical properties of the particles.

For the case of gel-trapped particles, 30 nm silica particles at 9 wt% were embedded in polyacrylamide hydrogels whose mesh size was varied by varying the crosslink density, with the latter characterized in terms of the gel storage modulus, *G*'. Results are plotted in Figure 5.4. The measured mobility μ_d was found to remain constant as the mesh size was decreased, i.e., as *G*' was increased, up to a value of 300 Pa, beyond which it decreased steeply. In a second set of measurements, silica particles with sizes ranging from 14 to 120 nm were imbedded in polyacrylamide gels with a constant storage modulus of approximately 100 Pa, corresponding to a mesh size of 6-11 nm.[22] As shown in figure 5.5. The measured mobility μ_d in these systems was found to be effectively constant, i.e., independent of the degree of trapping, as expressed by the ratio of the particle size to the mesh size. Thus for weak gels (*G*'<300Pa) probed at high frequency, the measured mobility was independent of the degree of trapping.

From a practical point of view the results show that electroacoustics can be used to measure the dynamic electrophoretic mobility of either un-trapped or trapped particles in viscoelastic gel media. In case of particles trapped in weak gels

(G'<300Pa) the degree of trapping experienced by the particle, as varied by either increasing crosslinker concentration (i.e. decreasing mesh size) at a constant particle size, or increasing particle size at a constant mesh size, did not alter the mobility significantly. It may be speculated that for such systems the interpretation of the μ_d measurements to yield particle electrical properties (zeta potential, etc.) might be effected by treating the background medium as a Newtonian liquid of suitable viscosity.

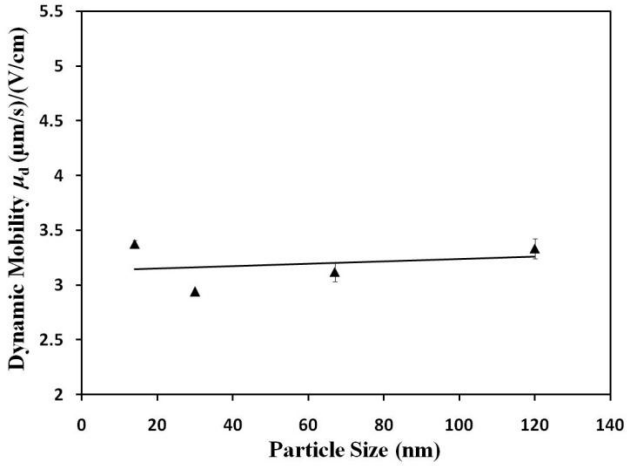

Figure 5.5: Dynamic electrophoretic mobility (μ_d) of different size silica particles trapped in 3 wt% polyacrylamide gels obtained with a 20:1 monomer-to-crosslinker ratio, and mobility measured at 80 min.

References

1. Laxton, P. B.; Berg, J. C., Colloid Aggregation Arrested by Caging within a Polymer Network. *Langmuir* **2008,** 24, (17), 9268-9272.

2. Hill, R. J., Electric-field-enhanced transport in polyacrylamide hydrogel nanocomposites. *Jr. Colloids & Int. Sci.* **2007,** 316, 635-644.

3. Wanga, M.; Hill, R. J., Electric-field-induced displacement of charged spherical colloids in compressible hydrogels. *Soft Matter* **2008,** 4, 1048-1058.

4. Grassmann, O.; Lobmann, P., Morphogenetic Control of Calcite Crystal Growth in Sulfonic Acid Based Hydrogels. *Chem. Eur. J.* **2003,** 9, (6), 1310-1316.

5. Grimm, A.; Nowak, C.; Hoffmann, J.; Schartl, W., Electrophoretic Mobility of Gold Nanoparticles in Thermoresponsive Hydrogels. *Macromolecules* **2009,** 42, (16), 6231–6238.

6. Dukhin, A. S.; Goetz, P. J., Acoustic Spectroscopy for Concentrated Polydisperse Colloids with Density Contrast. *Langmuir* **1996,** 12, (21), 4987-4997.

7. Dukhin, A. S.; Goetz, P. J., *Ultrasound for Characterizing Colloids*. Elsevier: 2002; Vol. 15.

8. Delgado, A. V.; González-Caballeroa, F.; Hunterb, R. J.; Koopalc, L. K.; Lyklema, J., Measurment and interpretation of electrokinetic phenomena. *Jr. Colloids & Int. Sci.* **2007,** 309, 194-224.

9. O'Brien, R. W., Electro-acoustic effects in a dilute suspension of spherical particles. *J. Fluid Mech.* **1988,** 190, 71-86.

10. Wang, M.; Hill, R. J., Dynamic electric-field-induced responce of charged spherical colloids in uncharged hydrogels. *J. Fluid Mech.* **2009,** 640, 357-400.

11. Mohammadi, A.; Hill, R. J., Dynamics of uncharged colloidal inclusions in polyelectrolyte hydrogels. *J. Fluid Mech.* **2010,** 669, 298–327.

12. Lamb, H., *Hydrodynamics*. 6th ed.; Dover: New York, 1945.

13. Urick, R. J., The Adbsorption of Sound in Suspensions of Irregular Particles. *J. Acoust. Soc. Am.* **1948,** 20, 283.

14. Busby, J.; Richardson, E. G., The Propogation of Ultrasonics in Suspensions of Particles in a Liquid. *Proc. Phys. Soc. (London)* **1956,** B69, 193.

15. Epstein, P. S.; Carhart, R. R., The Absorption of Sound in Suspensions and Emulsions I. Water Fog in Air. *J. Acoust. Soc. Am.* **1953,** 25, 553-565.

16. Allegra, J. R.; A., H. S., Attenuation of Sound in Suspensions and Emulsions: Theory and Experiments. *J. Acoust. Soc. Am.* **1972,** 51, (5), 1545-1564.

17. Gibson, R. L.; Toksoz, M. N., Viscous Attenuation of Acoustic Waves in Suspensions. *J. Acoust. Soc. Am.* **1989,** 85, (5), 1925-1934.

18. Hipp, A. K.; Storti, G.; Morbidelli, M., Particle Sizing in Colloidal Dispersions by Ultrasound. Model Calibration and Sensitivity Analysis. *Langmuir* **1999,** 15, (7), 2338-2345.

19. Weiner, M. L.; Kotkoskie, L. A., *Excipient Toxicity and Safety*. Marcel Dekker, Inc.: New York, 1999.

20. Wikipedia Hydroxypropyl cellulose. http://en.wikipedia.org/wiki/Hydroxypropyl_cellulose (July 7th 2010),

21. Bhosale, P. S.; Berg, J. C., Acoustic Spectroscopy of Colloids Dispersed in a Polymer Gel System. *Langmuir* **2010,** 26, (18), 14423–14426.

22. Russell, S. M.; Carta, G., Mesh Size of Charged Polyacrylamide Hydrogels from Partitioning Measurement. *Ind. Eng. Chem. Res.* **2005,** 44, 8213-8217.

SUMMARY & FUTURE DIRECTIONS

In this work we have investigated polymeric rheology modifiers for dense nuclear waste slurries using various macroscale (rheology and electroacoustics) and microscale (atomic force microscope) colloidal interaction measurement techniques. It was identified that polyelectrolytes, specifically poly (acrylic acid), are effective rheology modifiers for high pH and high salt content environments of nuclear waste slurries. Traditional non-ionic modifiers are not suitable due to low solvency and collapsed polymer conformation in these conditions. Poly (acrylic acid) adsorbs on all the major of oxide particle surfaces (Fe_2O_3, Al_2O_3, SiO_2, and ZrO_2) in the slurry. The adsorbed poly (acrylic acid) molecules steric stabilize these particles to prevent aggregation thus reducing yield stress and viscosity. Adsorption of poly (acrylic acid) also increases particle surface charge which increases electrostatic repulsion even at these high salt concentrations. In such systems physiochemical parameters like molecular weight, dosage, salt concentration, salt type, and pH need to be controlled for desired rheological performance.

It was found that the correct choice of molecular weight of the poly (acrylic acid) was especially important to its effectiveness. Salt concentration and salt type vary during dilution and concentration cycles in the processing plant. These changes can affect polymer conformation due to solvency effects and alter particle interactions from repulsive steric barrier to attractive bridging forces inducing aggregation. Aggregation of particles increases the yield stress and viscosity of the slurry. Since

polymer bridging is considered detrimental for the flow properties, it was further studied for a model system of silica particle suspensions flocculated by polyethylene oxide. A link between the dynamics of polymer bridge formation and disruption and its effect on flow behavior of particulate suspension was established. We have shown that the bridge flocculated colloidal gel can be destabilized by high shear mixing due to chain scission. Studies with acoustics and electroacoustics techniques have shown that such techniques are very useful for online characterization of the particle sedimentation and accumulation in the transport system. As a side project we have extended these techniques[1,2] to characterize particles dispersed in viscoelastic polymer gel media which is another complex system of interest. It was shown that electroacoustics can be used to directly measure the dynamic electrophoretic mobility of either un-trapped or trapped particles in viscoelastic gel media.

However, many unanswered questions and opportunities for discoveries remain. Studies with the model system of silica particle suspension flocculated with polyethylene oxide gave important insight into the dynamics of polymer bridge disruption and its effects on bulk rheology. The more relevant system for nuclear waste slurries is alumina suspensions flocculated by poly (acrylic acid). Silica – polyethylene oxide suspensions are shear thickening at low shears.[3] On application of sufficient shear, the polyethylene oxide desorbs from the particle surface and on this available free surface more polymer chains adsorb from the solution. These additionally adsorbed polymer chains connect the small aggregates in the dispersion, into a three-dimensional network spanning whole dispersion. The main condition for

forming such a network is that the adsorption energy of polyethylene oxide to the particle surface be lower than that of the entropic energy of polymer deformation.[4] This condition is not valid for the case of alumina -poly (acrylic acid) system. Poly (acrylic acid) adsorption is driven by strong chemisorption of carboxylic acid groups;[5] therefore bridge-flocculated aggregates are smaller, tighter and not well connected with each other. The rheological behavior of this suspension under shear is expected to be very different since the three-dimensional network of particles is not properly established in such a system. The smaller alumina-poly (acrylic acid) aggregates can also move against each other under shear, thus reducing the possibility of interparticle bond disruption and chain scission. Further studies are required to explore polymer bridging disruption dynamics and its effect on bulk rheology in such systems.

A simple analytical model quantitatively linking polymer bridging forces to bulk rheological properties, such as yield stress and storage modulus, needs to be designed. As a first step towards this goal, one can extend the model presented by Russel et al.[6] to the bridge flocculated particles. Interparticle interaction forces (F) for bridge flocculated particles can be calculated using a model presented by Sprakel et al.[7] or measured directly using AFM pull-off force measurements. However, a major challenge for designing such an analytical model is quantifying structural parameters in dense dispersions such as localization length of dense clusters or structural heterogeneity (flocculated vs. unflocculated particles) in the suspension. Structural information is critical to quantitatively correlating interparticle forces to the bulk rheological properties.[8]

The premise for all of the above studies was that particle aggregation, and the yield stress is detrimental to slurry transport. However, in many industrial systems like drilling mud and concrete suspensions the yield stress is desirable. The yield stress in these systems allows trapping, and transport of the larger particles (diameter > 100 μm) without settling. Nuclear waste slurries are also multiphase and contain solid particles ranging in size from few nm to few cm. A major challenge during transport is settling of heavy uranium particles. Potentially yield stress of the waste slurry can be used to trap large uranium particles and prevent settling. However, precise tuning of rheological properties will be required for such an application. Radiation induced degradation of polymeric rheology modifiers is also another practical challenge that needs to be addressed. These are just a few of the possibilities that could be expanded upon in the future.

References

1. Bhosale, P. S.; Berg, J. C., Poly(acrylic acid) as a rheology modifier for dense alumina dispersions in high ionic strength environments. *Colloids Surf., A: Physicochem. Eng. Aspects* **2010,** 362, (1-3), 71-76.

2. Bhosale, P. S.; Chun, J.; Berg, J. C., Electroacoustics of particles dispersed in polymer gel. *Langmuir* **2011,** 27, (12), 7376-7379.

3. Cabane, B.; Wong, K.; Lindner, P.; Lafuma, F., Shear induced gelation of colloidal dispersions. *Journal of Rheology* **1997,** 41, (3), 531-547.

4. Prasad, V. Weakly Interacting Colloid Polymer Mixtures. Harvard University, Cambridge, 2002.

5. Bhosale, P. S.; Chun, J.; Berg, J. C., Electrophoretic mobility of poly(acrylic acid)-coated alumina particles. *Jr. Colloids & Int. Sci.* **2011,** 258, 123-128.

6. Russel, W. B.; Saville, D. A.; Schowalter, W. R., *Colloidal Dispersions*. Cambridge Press 1989.

7. Sprakel, J.; Bartscherer, E.; Hoffmann, G.; Stuart, M. A. C.; Gucht, J. v. d., Dynamics of polymer bridge formation and disruption. *Phys. Rev. E* **2008,** 78, 0402802.

8. Mewis, J.; Wagner, N. J., *Colloidal Suspension Rheology*. Cambridge University Press: New York, 2012.

BIBLIOGRAPHY

1. Allegra, J. R.; Hawley, S. A., Attenuation of Sound in Suspensions and Emulsions: Theory and Experiments. *J. Acoust. Soc. Amer.* 1972, 51, (5), 1545-1564.

2. Barnes, H. A., A Handbook of Elementary Rheology. University of Wales Institute of Non-Newtonian Fluid Mechanics: 2000.

3. Berg, J. C., An Introduction to Interfaces and Colloids: The Bridge to Nanoscience. World Scientific 2010; p p. 616.

4. Bhosale, P. S.; Berg, J. C., Poly(acrylic acid) as a rheology modifier for dense alumina dispersions in high ionic strength environments. *Colloids Surf., A: Physicochem. Eng. Aspects* 2010, 362, (1-3), 71-76.

5. Bhosale, P. S.; Berg, J. C., Acoustic Spectroscopy of Colloids Dispersed in a Polymer Gel System. *Langmuir* 2010, 26, (18), 14423–14426.

6. Bhosale, P. S.; Berg, J. C., The dynamics of polymer bridge formation and disruption and its effect on the bulk rheology of suspensions. *Langmuir* 2012, in press.

7. Bhosale, P. S.; Chun, J.; Berg, J. C., Electrophoretic mobility of poly(acrylic acid)-coated alumina particles. *Jr. Colloids & Int. Sci.* 2011, 258, 123-128.

8. Bhosale, P. S.; Chun, J.; Berg, J. C., Electroacoustics of particles dispersed in polymer gel. *Langmuir* 2011, 27, (12), 7376-7379.

9. Bonacucinaa, G.; Cespia, M.; Palmieri, G. F., Evaluation of dissolution kinetics of hydrophilic polymers by use of acoustic spectroscopy. *International Journal of Pharmaceutics* 2009, 377, (1-2), 153-158.

10. Brown, W. P. http://www.docbrown.info/page07/transition06Fe.htm (Oct 4th 2011),

11. Buchholz, B. A.; Zahn, J. M.; Kenward, M.; Slater, G. W.; Barron, A. E., Flow-induced chain scission as a physical route to narrowly distributed, high molar mass polymers. *Polymer* 2004, 45, (4), 1223-1234.

12. Bulychev, N.; Dervaux, B.; Dirnberger, K.; Zubov, V.; Du Prez, F. E.; Eisenbach1, C. D., Structure of adsorption layers of amphiphilic copolymers on inorganic or organic particle surfaces. *Macromolecular Chemistry and Physics* 2010, 211, 971-976.

13. Busby, J.; Richardson, E. G., The Propogation of Ultrasonics in Suspensions of Particles in a Liquid. *Proc. Phys. Soc.* (London) 1956, B69, 193.

14. Cabane, B.; Wong, K.; Lindner, P.; Lafuma, F., Shear induced gelation of colloidal dispersions. *Journal of Rheology* 1997, 41, (3), 531-547.

15. Carasso, M. L.; Rowlands, W. N.; O'brien, R. W., The effect of neutral polymer and nonionic surfactant adsorption on the electroacoustic signals of colloidal silica. *Jr. Colloids & Int. Sci.* 1997, 193, (2), 200-214.

16. Cesarano, J.; Aksay, I. A., Processing of highly concentrated aqueous a-alumina suspension stablized with polyelectrolytes. *J. Am. Ceram. Soc.* 1988, 71, (12), 1062-1067.

17. Chang, H. O., Hazardous and radioactive waste treatment technologies handbook. CRC Press LLC: Florida, 2001.

18. Chibowski, S.; Mazur, E. O.; Patkowski, J., Influence of ionic strength on the adsorption properties of the system dispersed aluminium oxide-polyacrylic acid. *Mater. Chem. Phys.* 2005, 93, 262-271.

19. Chibowski, S.; Wis´niewska, M., Study of electrokinetic properties and structure of adsorbed layers of polyacrylic acid and polyacrylamide at Fe2O3–polymer solution interface. *Colloids Surf., A: Physicochem. Eng. Aspects* 2002, 208, 131-145.

20. Chibowski, S.; Wiśniewska, M., Study of the adsorption mechanism and structure of adsorbed layers of polyelectrolytes at metal oxide/solution interface. *Adsorpt. Sci. Tech*. 2001, 19, (5), 409-421.

21. Chun, J.; Poloski, A. P.; Hansen, E. K., Stabilization and Control of Rheological Properties of Fe2O3-rich Colloidal Slurries under High Ionic Strength and pH. *Jr. Colloids & Int. Sci.* 2010, 348, (1), 280-288.

22. Cliftona, M.; Nguyena, T.; Frost, R., Effect of ionic surfactants on bauxite residues suspensions viscosity. *Jr. Colloids & Int. Sci.* 2007, 307, 572-577.

23. Colic, M.; Franks, G. V.; Fisher, M. L.; Lange, F. F., Effect of Counterion Size on Short Range Repulsive Forces at High Ionic Strengths. *Langmuir* 1997, 13, (12), 3129-3135.

24. Das, K. K.; Somasundaran, P., Ultra-low dosage flocculation of alumina using polyacrylic acid. Colloids Surf., A: Physicochem. Eng. Aspects 2001, 182, 25-33.

25. Das, K. K.; Somasundaran, P., Flocculation-dispersion characteristics of alumina using a wide molecular weight range of polyacrylic acids. *Colloids Surf., A: Physicochem. Eng. Aspects* 2003, 223, 17-25.

26. Dasgupta, B. R.; Weitz, D. A., Microrheology of cross-linked polyacrylamide networks. *Phys. Rev. E 2005*, 71, (021504).

27. Delgado, A. V.; González-Caballeroa, F.; Hunterb, R. J.; Koopalc, L. K.; Lyklema, J., Measurment and interpretation of electrokinetic phenomena. J*r. Colloids & Int. Sci.* 2007, 309, 194-224.

28. Dijt, J. C.; Cohen Stuart, M. A.; Fleer, G. J., Kinetics of polymer adsorption and desorption in capillary flow. *Macromolecules* 1992, 25, (20), 5416-5423.

29. Dukhin, A.; Dukhin, S.; Goetz, P., Electrokinetics at high ionic strength and hypothesis of the double layer with zero surface charge. *Langmuir* 2005, 21, 9990-9997.

30. Dukhin, A. S.; Goetz, P. J., Acoustic Spectroscopy for Concentrated Polydisperse Colloids with Density Contrast. *Langmuir* 1996, 12, (21), 4987-4997.

31. Dukhin, A. S.; Goetz, P. J., Acoustic Spectroscopy for Concentrated Polydisperse Colloids with Density Contrast. *Langmuir* 1996, 12, (21), 4987-4997.

32. Dukhin, A. S.; Goetz, P. J., Ultrasound for Characterizing Colloids. Elsevier: Amsterdam, 2002; Vol. 15.

33. Edwards, S. F.; Vilgis, T. A., The Tube Model Theory of Rubber Elasticity. *Rep. Prog. Phys.* 1988, 51, 243-297.

34. Epstein, P. S.; Carhart, R. R., The Absorption of Sound in Suspensions and Emulsions I. Water Fog in Air. *J. Acoust. Soc. Amer.* 1953, 25, 553-565.

35. Fleer, G. J.; Cohen Stuart, M. A.; Scheutjens, J. M. H. M.; Cosgrove, T.; Vincent, B., Polymers at interfaces. Chapman & Hall Inc.: New York, 1993.

36. Frens, G., Interacting Particles in Contact. *Faraday Discuss. Chem. Soc.* 1990, 90, 143-151.

37. Gebhardt, J. E.; Fuerstenau, D. W., Adsorption of Polyacrylic acid at oxide/water interfaces. *Colloids and Surfaces* 1983, 7, 221-231.

38. Gibson, R. L.; Toksoz, M. N., Viscous Attenuation of Acoustic Waves in Suspensions. *J. Acoust. Soc. Amer.* 1989, 85, (5), 1925-1934.

39. Grassmann, O.; Lobmann, P., Morphogenetic Control of Calcite Crystal Growth in Sulfonic Acid Based Hydrogels. *Chem. Eur. J.* 2003, 9, (6), 1310-1316.

40. Grassmann, O.; Löbmann, P., Biomimetic nucleation and growth of CaCO3 in hydrogels incorporating carboxylate groups. *Biomaterials* 2004, 25, (2), 277-282

41. Greenwood, R., Review of the measurement of zeta potentials in concentrated aqueous suspensions using electroacoustics. *Advances in Colloid and Interface Science* 2003, 106, 55-81.

42. Greenwood, R.; Kendall, K., Effect of ionic strength on the adsorption of cationic polyelectrolytes onto alumina studied using electroacoustic measurements. *Powder Technology* 2000, 113, (1-2), 148-157.

43. Gregory, J., Polymer Flocculation In Flowing Dispersions. Academic Press: London, 1982.

44. Grimm, A.; Nowak, C.; Hoffmann, J.; Schartl, W., Electrophoretic Mobility of Gold Nanoparticles in Thermoresponsive Hydrogels. *Macromolecules* 2009, 42, (16), 6231–6238.

45. Hierrezuelo, J.; Sadeghpour, A.; Szilagyi, I.; Vaccaro, A.; Borkovec, M., Electrostatic stabilization of charged colloidal particles with adsorbed polyelectrolytes of opposite charge. *Langmuir* 2010, 26, (19), 15109-15111.

46. Hill, R. J., Electric-field-enhanced transport in polyacrylamide hydrogel nanocomposites. *Jr. Colloids & Int. Sci.* 2007, 316, 635-644.

47. Hill, R. J.; Saville, D. A., 'Exact' solutions of the full electrokinetic model for soft spherical colloids: Electrophoretic mobility. *Colloids Surf., A: Physicochem. Eng. Aspects* 2005, 267, (1-3), 31-49.

48. Hill, R. J.; Saville, D. A.; Russel, W. B., Electrophoresis of spherical polymer-coated colloidal particles. *Jr. Colloids & Int. Sci.* 2002, 258, (1), 56-74.

49. Hipp, A. K.; Storti, G.; Morbidelli, M., Particle Sizing in Colloidal Dispersions by Ultrasound. Model Calibration and Sensitivity Analysis. *Langmuir* 1999, 15, (7), 2338-2345.

50. Huang, A. Y.; Berg, J. C., High-salt stabilization of laponite clay particles. *Jr. Colloids & Int. Sci.* 2006, 296, (1), 159-164.

51. Israelachvili, J. N., Intermolecular and Surface Forces. Third ed.; Academic Press: 2011.

52. Kauzmann, W.; Eyring, H., The Viscous Flow of Large Molecules. *Journal of the American Chemical Society* 1940, 62, (11), 3113-3125.

53. Kay, E. D.; Calloway, T. B.; Koopman, D. C.; Brigmon, R. L.; Eibling, R. E., Rheology modifiers for radioactive waste slurries. Proc. ASME Fluid Eng. Div. Summer Meeting 2003 4549.

54. Kirwan, L. J.; Fawell, P. D.; Bronswijk, W. V., An in situ FTIR-ATr study of polyacrylate adsorbed onto hematite at high pH and high ionic strength. *Langmuir* 2004, 20, (10), 4093-4100.

55. Kosmulski, M.; Rosenholm, J. B., High ionic strength electrokinetics. *Advances in Colloid and Interface Science* 2004, 112, 93-107.

56. Lamb, H., Hydrodynamics. 6th ed.; Dover: New York, 1945.

57. Larson, R. G., Structure and Rheology of Complex Fluids. Oxford University Press: New York 1999; p p.351.

58. Larson, R. G., Structure and Rheology of Complex Fluids. Oxford University Press: New York 1999; p p.351.

59. Laxton, P. B.; Berg, J. C., Colloid Aggregation Arrested by Caging within a Polymer Network. *Langmuir* 2008, 24, (17), 9268-9272.

60. Levine, A. J.; Lubensky, T. C., Response function of a sphere in a viscoelastic two-fluid medium. *Physical Review E* 2001, 63, (041510).

61. Lewis, J. A., Gel casting and dense colloidal slurries. *J. Acoust. Soc. Amer.* 2004, 83, (10), 2341-2359.

62. Li, Q.; Lewis, J. A., Nanoparticle Inks for Directed Assembly of Three-Dimensional Periodic Structures. *Advanced Materials* 2003, 15, (19), 1639–1643.

63. Li, Q.; Lewis, J. A., Nanoparticle Inks for Directed Assembly of Three-Dimensional Periodic Structures. *Advanced Materials* 2003, 15, (19), 1639-1643.

64. Liétor-Santos, J. J.; Fernández-Nieves, A., Electrophoresis of large polyelectrolyte-coated colloidal particles. *Phys. Rev. E* 2005, 71, 042401.

65. Lu, K.; Kessler, C., Nanoparticle colloidal suspension optimization and freeze-cast forming. *Ceram. Eng. Sci. Proc.* 2006, 27, (8), 1-10.

66. Lu, P. J.; Zaccarelli, E.; Ciulla, F.; Schofield, A. B.; Sciortino, F.; Weitz, D. A., Gelation of particles with short range attraction. *Nature* 2008, 453, 499-503

67. Maier, H.; Baker, J. A.; Berg, J. C., The effect of adsorbed polymers on the ESA potential of aqueous silica dispersions. *Jr. Colloids & Int. Sci.* 1987, 119, (2), 512-517.

68. Mason, T. G.; Weitz, D. A., Optical measurements of frequency-dependent linear viscoelastic moduli of complex fluids. *Phys. Rev. Lett.* 1995, 74, (7), 1250-1253.

69. Matos, M. A.; White, L. R.; Tilton, R. D., Electroosmotically enhanced mass transfer through polyacrylamide gels. *Macromolecules* 2006, 41, (19), 7194–7202.

70. Matos, M. A.; White, L. R.; Tilton, R. D., Enhanced mixing in polyacrylamide gels containing embedded silica nanoparticles as internal electro-osmotic pumps. *Colloids Surf. B* 2008, 61, (2), 262–269.

71. Menga, B.; Wua, J.; Li, Y.; Loua, L., Aging process of the bond between colloidal particles measured using laser tweezers. *Colloids Surf., A: Physicochem. Eng. Aspects* 2008, 322, 253-255.

72. Mewis, J.; Wagner, N. J., Current trends in suspension Rheology. *J. Non-Newtonian Fluid Mech.* 2009, 157, 147-150.

73. Miling, A. J.; Vincent, B., Depletion forces between silica surfaces in solution of poly(acryic acid) *J. Chem. Soc., Faraday Trans.* 1997, 93, (17), 3179-3183.

74. Milkova, V.; Kamburova, K.; Radeva, T.; Stoimenova, M., Electrical properties of polyelectrolyte layers adsorbed on colloidal particles at different ionic strengths *Langmuir* 2010, 26, (18), 14488-14493.

75. Miller, N. P.; Berg, J. C., A comparison of electroacoustic and microelectrophoretic zeta potential data for titania in the absence and presence of a poly (vinyl alcohol) adlayer. *Colloids and Surfaces* 1991, 59, (8), 119-128.

76. Mohammadi, A.; Hill, R. J., Dynamics of uncharged colloidal inclusions in polyelectrolyte hydrogels. *J. Fluid Mech.* 2010, 669, 298–327.

77. Napper, D. H., Polymeric stabilization of colloidal dispersions. Academic Press Inc.: New York, 1983.

78. Napper, D. H., Polymeric stabilization of colloidal dispersions. Academic Press Inc.: New York, 1983.

79. Nguyen, T. Q., Dynamics of Flexible Polymer Chains in Elongational Flow CHIMIA 2001, 55, (3), 147-154.

80. Nguyen, T. Q.; Kausch, H. H., Effects of solvent viscosity on polystyrene degradation in transient elongational flow. *Macromolecules* 1990, 23, (24), 5137-5145.

81. O'Brien, R. W., Electro-acoustic effects in a dilute suspension of spherical particles. *Journal of Fluid Mechanics* 1988, 190, 71-86.

82. O'Brien, R. W., Electro-acoustic effects in a dilute suspension of spherical particles. *J. Fluid Mech.* 1988, 190, 71-86.

83. O'Brien, R. W., The effect of an absorbed polyelectrolyte layer on the dynamic mobility of a colloidal particle. *Particle and Particle Systems Characterization* 2002, 19, (3), 186-194.

84. O'Brien, R. W.; Beattie, J. K.; Hunter, R. J., Particle Characterization Using Electro-Acoustic Spectroscopy. Wiley-VCH Verlag GmbH & Co. KGaA: Weinheim, 2008.

85. Ohshima, H., Electrophoresis of Soft Particles. *Advances in colloid and interface science* 1995, 62 189-235.

86. Palmqvista, L.; Lyckfeldta, O.; Carlströma, E.; Davoustb, P.; Kauppic, A.; Holmbergd, K., Dispersion mechanisms in aqueous alumina suspensions at high solids loadings. *Colloids Surf., A: Physicochem. Eng. Aspects* 2006, 274, 100-109

87. Palmqvista, L.; Lyckfeldta, O.; Carlströma, E.; Davoustb, P.; Kauppic, A.; Holmbergd, K., Dispersion mechanisms in aqueous alumina suspensions at high solids loadings. *Colloids Surf., A: Physicochem. Eng. Aspects* 2006, 274, 100-109

88. Pamqvist, L.; Holmberg, K., Dispersant adsorption and viscoelasticity of alumina suspensions measured by quartz crystal microbalance with dissipation monitoring and in situ dynamic rheology. *Langmuir* 2008, 24, (18), 9989-9996.

89. Pamqvista, L.; Holmberg, K., Dispersant adsorption and viscoelasticity of alumina suspensions measured by quartz crystal microbalance with dissipation monitoring and in situ dynamic rheology. *Langmuir* 2008, 24, (18), 9989-9996.

90. Patel, P. D.; Russel, W. B., The rheology of polystyrene latexes phase separated by dextran. *Journal of Rheology* 1987, 31, (7), 599-618.

91. Prabhakaran, K.; Sooraja, R.; Melkeria, A.; Gokhalea, N. M.; Sharmaa, S. C., A new direct coagulation casting process for alumina slurries prepared using poly(acrylate) dispersant. *Ceram. Int.* 2009, 35, (3), 979-985

92. Russel, W. B.; Saville, D. A.; Schowalter, W. R., Colloidal Dispersions. Cambridge Press 1989.

93. Russell, S. M.; Carta, G., Mesh Size of Charged Polyacrylamide Hydrogels from Partitioning Measurement. *Ind. Eng. Chem. Res.* 2005, 44, 8213-8217.

94. Sarkar, D.; Somasundaran, P., Conformational dynamics of poly(acrylic acid). A study using surface plasmon resonance spectroscopy. *Langmuir* 2004, 20, (11), 4657-4664.

95. Sim, H. G.; Khomami, B.; Sureshkumar, R., Flow--induced chain scission in dilute polymer solutions: Algorithm development and results for scission dynamics in elongational flow. *Journal of Rheology* 2007, 51, (6), 1223-1251.

96. Spitzer, D.; Dai, Q., Effect of flocculant molecular weight on rheology. *Light Metals* 2006, 11-15.

97. Squires, T. M.; Mason, T. G., Fluid Mechanics of Microrheology. *Annu. Rev. Fluid Mech.* 2010, 42, 413-438.

98. Staudinger, H., Isoprene and rubber. XX. Colloidal nature of rubber, gutta-percha and balata. Berichte der Deutschen Chemischen Gesellschaft [Abteilung] B: Abhandlungen 1930, 63B, 921-934.

99. Staudinger, H.; Heuer, W., Highly polymerized compounds. XCIII. The breaking up of the molecular fibers of the polystyrenes Berichte der Deutschen Chemischen Gesellschaft [Abteilung] B: Abhandlungen 1934, 67B, 1159-1164.

100. Staudinger, H.; Leupold, E. O., Isoprene and rubber. XVIII. Studies of the viscosity of balata. Berichte der Deutschen Chemischen Gesellschaft [Abteilung] B: Abhandlungen 1930, 63B, 730-733.

101. Stenkamp, V. S.; McGuiggan, P. M.; Berg, J. C., Restabilization of Electrosterically Stabilized Colloids in High Salt Media. *Langmuir* 2001, 17, (3), 637–651.

102. Stumm, W., Chemistry of Solid-Water Interface. John Wiley & Sons, Inc.: New York, 1992.

103. Thompson, J. W.; Stretz, H. A.; Arce, P. E., Preliminary Observations of the Role of Material Morphology on Protein-Electrophoretic Transport in Gold Nanocomposite Hydrogels. *Ind. Eng. Chem. Res.* 2010, 49, (23), 12104–12110.

104. Urick, R. J., The Adbsorption of Sound in Suspensions of Irregular Particles. *J. Acoust. Soc. Amer.* 1948, 20, 283.

105. Vakarelski, I. U.; Ishimura, K.; Higashitani, K., Adhesion between Silica Particle and Mica Surfaces in Water and Electrolyte Solutions. *Jr. Colloids & Int. Sci.* 2000, 227, (1), 111-118.

106. Wang, M.; Hill, R. J., Dynamic electric-field-induced responce of charged spherical colloids in uncharged hydrogels. *J. Fluid Mech.* 2009, 640, 357-400.

107. Wanga, M.; Hill, R. J., Electric-field-induced displacement of charged spherical colloids in compressible hydrogels. *Soft Matter* 2008, 4, 1048-1058.

108. Weiner, M. L.; Kotkoskie, L. A., Excipient Toxicity and Safety. Marcel Dekker, Inc.: New York, 1999.

109. Wikipedia Hydroxypropyl cellulose. http://en.wikipedia.org/wiki/Hydroxypropyl_cellulose (July 7th 2010),

110. Wiśniewska, M.; Chibowskia, S.; Urbana, T., Adsorption and thermodynamic properties of the alumina–polyacrylic acid solution system. *Jr. Colloids & Int. Sci.* 2009, 334, (2), 146-152.

111. Yilmaza, H.; Satoa, K.; Wataria, K., AFM interaction study of α-alumina particle and c-sapphire surfaces at high-ionic-strength electrolyte solutions. *Jr. Colloids & Int. Sci.* 2007, 307, (1), 116-123.

112. Zhang, J.; Xu, Q.; Tanaka, H.; Iwasa, M., Improvement of Dispersion of Al2O3 slurries using EDTA-4Na. *J. Am. Ceram. Soc.* 2006, 89, (4), 1440-1442.9, (4), 1440-1442.

APPENDIX I

Colloidal Probe Atomic Force Microscopy

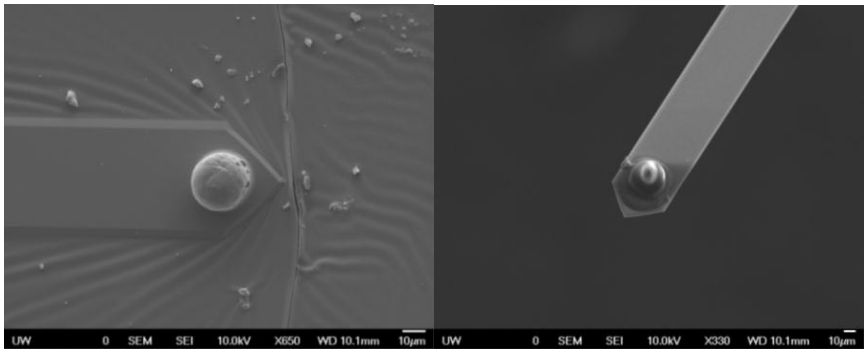

Figure 1: Electron micrographs of alumina (left) and glass (right) particles glued to probe tips (scale bar 10 μm).

Atomic force microscopy z-force measurement provides a simple and powerful technique to quantify net surface and adhesion forces. This method is also commonly referred as colloid force microscopy. In this work the technique is used to measure adhesion forces between various oxide particles in liquid environments similar to those of nuclear waste slurries. In such systems, a well characterized piezocrystal is used to measure the relative surface separation distance, while the deflection in the cantilever spring measures the interaction forces. From a practical standpoint, AFM has unique advantages over SFA, as the particle of interest can be attached to the cantilever, and the surface of choice can be used to measure interaction forces.[11]

In chapter 3 The long range electrostatic repulsion, and short range adhesion forces between an alumina particle against a sapphire surface and a glass particle against a silica wafer in various KNO_3 solutions (0.001-0.5M) and in the supernatant

of the nuclear waste simulant AZ101. Sapphire and silicon wafers are obtained from the University Wafers Corp., Boston, MA. Glass microspheres of 10-20μm and alumina microspheres of 20 -25μm (DAW 45) are obtained from Duke Scientific, Palo Alto, CA and Denka Corp., (New York, NY) respectively. Tip-less cantilevers probes (0.2 to 0.6 N/m) are purchased from Nanoscience Instruments, (Phoenix, AZ). Nuclear waste stimulant AZ 101 is provided by Pacific Northwest National Laboratory, (Richland, WA). All other chemicals: DI ultra-filtered water, acetone, ethanol, KNO_3 were purchased from Fisher Scientific, (Pittsburg, PA).

Cleaning Procedures

The sapphire and silicon wafers are rinsed using water/acetone/ethanol/water followed by drying under N_2 gas and UV cleaned for 20 min in a UV Procleaner system by Bioforce Nanoscience Corp., (Ames, IA). The particles are cleaned using water/acetone/ethanol/water and dried before attaching to the probe. Before each experiment the probe with the particle is UV cleaned for 20 min. All the glassware used is cleaned in a base bath and then rinsed thoroughly by DI ultra filtered water. All the force distance measurements are conducted using a diCaliber scanning probe microscope (Veeco Instruments Inc., Plainview, NY). A single microsphere (glass/alumina) is attached to the silicon AFM tip (spring constant 0.2-0.6 N/m) using 5 min epoxy from ITW Devcon (Danvers, MA). The attached particle is imaged using JSM7000F scanning electron microscope (JEOL Ltd., Tokyo, Japan) to measure

particle size. The resonance frequency of the cantilever is measured before (v_o) and after (v_1) the particle attachment which is then used in Cleveland method[12] for calibrating spring constant

$$C_N = \frac{(2\pi)^2 M_1}{(1-\nu_1^2)(1-\nu_0^2)} \tag{4.1}$$

where M_1 is particle mass. For all the experiments the ramp rate is maintain at 50 nm/s.

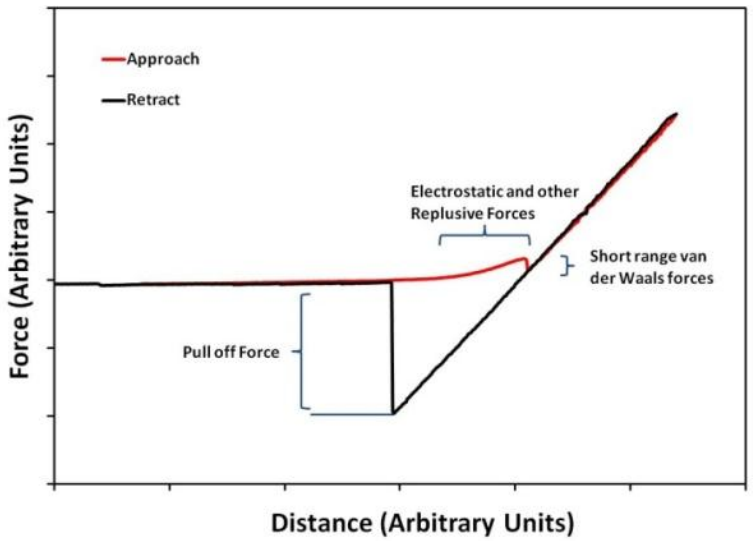

Figure 2: A typical approach (red) and retraction (black) force distance curves obtained from the atomic force microscope instrument.

Figure 1 shows an alumina and a glass sphere attached to the tipless cantilever beam. Figure 2 shows typical force-distance curves as the probe approaches and retracts from the surface. The interaction forces are typically measured in terms of the photodiode signal in Volts or Amps, which are converted into actual force (nN or mN) using the cantilever spring constant (C_N). As the probe approaches the surface, the

long range surface forces like electrostatic repulsion bends the cantilever represented by upward bend in the force distance curve. When the probe gets close enough to the surface attractive van der Waals forces dominate, and the probe is drawn to the surface in that is termed snap- in. The snap-in is followed by a linear defection in the cantilever spring. The point of snap-in or the point at which linear cantilever deflection starts is considered zero separation distance. During retraction the adhesion forces between the particle and the surface are measured by snap-out or puff-off force, which represents the amount of cantilever deflection before particle comes out of contact. For a well calibrated piezocrystal system, the photodiode signal *vs.* distance curve measured is then converted into a normalized force per unit radius F/R (mN/m) *vs.* relative separation distance. The photodiode signal is converted into force using

$$\frac{F}{R} = \frac{V}{RS} C_N \qquad (4.2)$$

where V is amount of deflection in Volts or Amps, constant S is the slope of the linear deflection line (Volts or Amps/nm), R is the probe radius (nm) and C_N is spring constant (N/m). Figure 3 shows the normalized force-distance curve for an alumina particle against a sapphire surface in DI water. The electrostatic repulsion forces and the van der Waals forces are measured in the approach curve, and on retraction, adhesion between the alumina surfaces is shown.

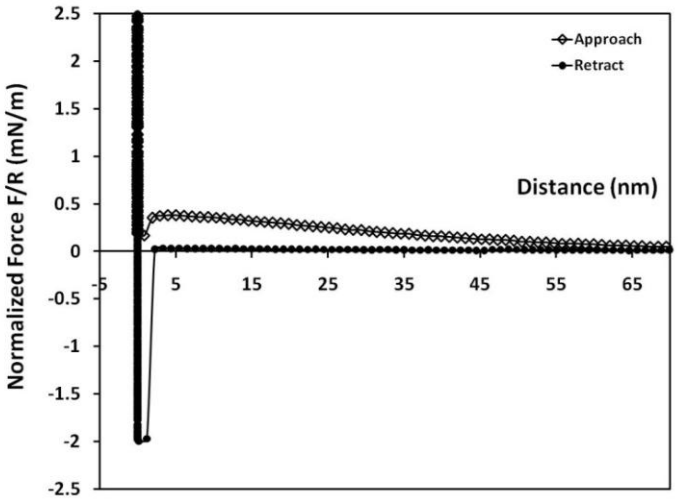

Figure 3: Interaction forces (*F*) normalized by probe radius (*R*) plotted against relative surface separation distance for alumina particle against sapphire surface in DI water.